Published for SISSA by Springer

Received: *September 3, 2018*
Accepted: *November 21, 2018*
Published: *December 11, 2018*

$\mathcal{N} = (0, 2)$ SYK, chaos and higher-spins

Cheng Peng

Department of Physics, Brown University,
Providence RI 02912, U.S.A.

E-mail: cheng_peng@brown.edu

Abstract: We study a 2-dimensional SYK-like model with $\mathcal{N} = (0, 2)$ supersymmetry. The model describes N chiral supermultiplets and M Fermi supermultiplets with a $(q+1)$-field interaction. We solve the model analytically and numerically in the $N \gg 1$, $M \gg 1$ limit with $\mu \equiv \frac{M}{N}$ being a free parameter. Two distinct higher-spin symmetries emerge when the μ parameter approaches the two ends of its range. This is verified by the appearance of conserved higher-spin operators and the vanishing of chaotic behaviors in the two limits. Therefore this model provides a manifest realization of the widely believed connection between SYK-like models and higher-spin theories. In addition, as the parameter μ varies we find the largest Lyapunov exponent of this model to be slightly larger than that in models with non-chiral supersymmetry.

Keywords: 1/N Expansion, Extended Supersymmetry, Higher Spin Symmetry, Conformal Field Theory

ArXiv ePrint: 1805.09325

Open Access, © The Authors.
Article funded by SCOAP[3].

https://doi.org/10.1007/JHEP12(2018)065

JHEP12(2018)065

Contents

1 Introduction **1**

2 An $\mathcal{N} = (0, 2)$ supersymmetry SYK model **2**
- 2.1 Review of 2d $\mathcal{N} = (0, 2)$ supersymmetry 2
- 2.2 The $\mathcal{N} = (0, 2)$ SYK model 4

3 Four-point functions **6**
- 3.1 Operator spectrum 7
- 3.2 Chaotic behavior 11

4 Two higher-spin limits **14**
- 4.1 The $\mu q \to 1^+$ ("classical chiral") limit 15
- 4.2 The $\mu \to +\infty$ ("classical Fermi") limit 19
- 4.3 Relations with higher-spin theories 23

A 2d SYK model with $\mathcal{N} = (2, 2)$ supersymmetry **25**

B Perturbing the $\mathcal{N} = (2, 2)$ model to the $\mathcal{N} = (0, 2)$ models **27**

C Fermionic operators in the model **30**
- C.1 The $\bar{\phi}\psi$ and $\phi\bar{\psi}$ sector 30
- C.2 The $\bar{\phi}\lambda$ and $\phi\bar{\lambda}$ sector 32

1 Introduction

The Sachdev-Ye-Kitaev (SYK) model [1–7] provides a simple example of strongly coupled, yet perturbatvely solvable, models [4, 6–11]. A reparameterization symmetry emerges in the infrared of this model [5–7] and its breaking leads to soft modes that are described by a Schwarzian derivative action [5, 7, 9, 12–14]. The Schwarzian derivative action also describes dilaton gravity systems on near AdS_2 spacetimes [6, 7, 15–22]. In addition, the SYK model is chaotic [4–6, 23], which is also a characteristic feature of gravitational theories [24–27]. All these properties suggest a holographic duality between the SYK model and dilaton gravity theories [4–7, 18, 28, 29]. Properties of the Hilbert space of the SYK model are studied in [6, 8, 9, 30–38]. The operator spectrum of the model consists of a tower of operators with finite anomalous dimensions [5–8]. The finite anomalous dimensions suggest [6] that the SYK model could be thought of as a deformation of the vector models that have a tower of higher spin operators with small anomalous dimensions. Such deformation from a Gross-Neveu vector model to an SYK-like model is discussed explicitly in [39]. It is shown in [39] that there is a transition from the vector model to the SYK-like model, which is similar to other phase transitions observed in the SYK-like models [40–46]. Different bulk duals of the tower of operators are proposed in [10, 47–50], other discussions about the relations between the two sides can be found in [51–58]. Most

JHEP12(2018)065

of the analytic results of the SYK model are derived in a new type of large-N limit that is shared in particular by models without random couplings [59–97].

To understand the relations between the SYK model and other better known models, different generalizations of the SYK model are constructed. One generalization is to include supersymmetry [98–102]. Aspects of supersymmetric SYK models have also been studied in [98, 103–112]. Another generalization is to higher dimensions [101, 113–126], whose simplest example is in 2 dimension. Continuum theories in 2-dimensional Euclidean spacetime are usually studied in terms of the left- and right-moving sectors due to the factorization of the isometry. The examples of 2d SYK-like models studied previously are all symmetric between the left- and the right-moving sectors.

One could also consider models whose left- and right-moving sectors are not symmetric. In this paper we study some 2d SYK-like models of this kind. The models have an $\mathcal{N} = (0, 2)$ supersymmetry in the UV. In the infrared, these theories are dominated by the set of melonic diagrams in the large-N limit and can be solved as all other SYK-like models.

The $\mathcal{N} = (0, 2)$ supersymmetry plays an important role of this model. The $\mathcal{N} = 2$ supersymmetry in the right-moving sector makes the IR solution reliable. On the other hand the absent of supersymmetry in the left-moving sector gives some room for interesting properties that are not observed in previous models. In particular, due to the smaller number of supersymmetry it is possible to study a one parameter family of such models. As a result, one could move on the moduli space of such models and understand their peculiar features, as well as their possible connections with other well studied models. In this paper we study two examples of such interesting consequences.

Firstly, the Lyapunov exponent of the supersymmetric model considered in [101], see also [127], is $\lambda_L = 0.5824$, which does not saturate the chaotic bound [26]. It is then an interesting question to ask if there are other 2d SYK-like models that have larger or maximal Lyapunov exponent. In this paper, we show that in our $\mathcal{N} = (0, 2)$ setting, as we dial the free parameter, there is a continuous family of theories that have slightly larger Lyapunov exponent comparing to the supersymmetric models considered in [101]. This is discussed in detail in section 3.2.

Another interesting consequence is the existence of certain higher-spin limits. By continuously tune the parameter to some limiting values, we observe the emergence of higher-spin conserved currents explicitly. Besides, we observe the correlation of the emerging of the higher-spin symmetry and the fading of the chaotic behavior. This provides a manifestation of a connection between higher-spin like models and SYK-like models. The details of such higher-spin limits are analyzed in section 4.

2 An $\mathcal{N} = (0, 2)$ supersymmetry SYK model

2.1 Review of 2d $\mathcal{N} = (0, 2)$ supersymmetry

In this section we review some properties of 2-dimensional theories with $\mathcal{N} = (0, 2)$ supersymmetry. We work in Euclidean signature, where the two coordinates are x^0, x^1.

JHEP12(2018)065

We define

$$z \equiv x^0 + ix^1\,, \qquad \bar{z} \equiv x^0 - ix^1\,, \tag{2.1}$$

and the derivatives become

$$\partial_z = \frac{1}{2}(\partial_0 - i\partial_1)\,, \qquad \partial_{\bar{z}} = \frac{1}{2}(\partial_0 + i\partial_1)\,. \tag{2.2}$$

The $\mathcal{N} = (0,2)$ supersymmetry is generated by 2 supercharges. In the superspace formalism they read

$$Q_+ = \frac{\partial}{\partial\theta^+} - 2\bar{\theta}^+\partial_z\,, \qquad \bar{Q}_+ = -\frac{\partial}{\partial\bar{\theta}^+} + 2\theta^+\partial_z\,. \tag{2.3}$$

The super-derivatives are

$$D_+ = \frac{\partial}{\partial\theta^+} + 2\bar{\theta}^+\partial_z\,, \qquad \bar{D}_+ = -\frac{\partial}{\partial\bar{\theta}^+} - 2\theta^+\partial_z\,. \tag{2.4}$$

It is easy to check that the supercharges anticommute with the super-derivatives.

We consider models of two kinds of superfields. The chiral/anti-chiral superfields

$$\Phi = \phi + \sqrt{2}\theta^+\psi + 2\theta^+\bar{\theta}^+\partial_z\phi\,, \qquad \bar{\Phi} = \bar{\phi} - \sqrt{2}\bar{\theta}^+\bar{\psi} - 2\theta^+\bar{\theta}^+\partial_z\bar{\phi}\,, \tag{2.5}$$

satisfy

$$\bar{D}_+\Phi = 0\,, \qquad D_+\bar{\Phi} = 0\,. \tag{2.6}$$

We also consider Fermi multiplets

$$\Lambda = \lambda - \sqrt{2}\theta^+ G + 2\theta^+\bar{\theta}^+\partial_z\lambda - \sqrt{2}\bar{\theta}^+ E \tag{2.7}$$

$$\bar{\Lambda} = \bar{\lambda} - \sqrt{2}\bar{\theta}^+\bar{G} - 2\theta^+\bar{\theta}^+\partial_z\bar{\lambda} - \sqrt{2}\theta^+\bar{E}\,, \tag{2.8}$$

where

$$E(\Phi) = E(\phi_a) + \sqrt{2}\theta^+\frac{\partial E}{\partial\phi_a}\psi_a + 2\theta^+\bar{\theta}^+\partial_{\bar{z}}E(\phi_a) \tag{2.9}$$

$$\bar{E}(\Phi) = \bar{E}(\bar{\phi}_a) + \sqrt{2}\bar{\theta}^+\frac{\partial\bar{E}}{\partial\bar{\phi}_a}\bar{\psi}_a - 2\theta^+\bar{\theta}^+\partial_{\bar{z}}\bar{E}(\bar{\phi}_a)\,, \tag{2.10}$$

are (anti-)chiral superfields where the subscript a labels different chiral superfields. The Fermi supermultiplets satisfy

$$\bar{D}_+\Lambda = \sqrt{2}E\,, \qquad \bar{D}_+E = 0\,, \tag{2.11}$$

$$D_+\bar{\Lambda} = \sqrt{2}\bar{E}\,, \qquad D_+\bar{E} = 0\,. \tag{2.12}$$

The supersymmetry transformation of the fields in the chiral supermultiplet is

$$Q_+\phi = \sqrt{2}\psi\,, \quad Q_+\psi = 0\,, \quad \bar{Q}_+\phi = 0\,, \quad \bar{Q}_+\psi = -2\sqrt{2}\partial_z\phi \tag{2.13}$$

$$\bar{Q}_+\bar{\phi} = \sqrt{2}\bar{\psi}\,, \quad \bar{Q}_+\bar{\psi} = 0\,, \quad Q_+\bar{\phi} = 0\,, \quad Q_+\bar{\psi} = -2\sqrt{2}\partial_z\bar{\phi}\,. \tag{2.14}$$

JHEP12(2018)065

The supersymmetry transformation of the fields in the Fermi supermultiplet is

$$Q_+\lambda = -\sqrt{2}G\,, \qquad Q_+G = 0\,, \quad \bar{Q}_+\lambda = \sqrt{2}E\,, \qquad \bar{Q}_+G = 2\sqrt{2}\partial_z\lambda + \frac{\partial E}{\partial\phi_a}\psi_a\,, \tag{2.15}$$

$$\bar{Q}_+\bar{\lambda} = \sqrt{2}\bar{G}\,, \qquad \bar{Q}_+\bar{G} = 0\,, \quad Q_+\bar{\lambda} = -\sqrt{2}\bar{E}\,, \qquad Q_+\bar{G} = -2\sqrt{2}\partial_z\bar{\lambda} + \frac{\partial\bar{E}}{\partial\bar{\phi}_a}\bar{\psi}_a\,. \tag{2.16}$$

In the rest of the paper we consider special models with $E = 0$.

Given these transformations, propagators of the different components of a chiral supermultiplet are related by

$$G^{\psi}(z_1, z_2) = -2\partial_{z_1}G^{\phi}(z_1, z_2) = 2\partial_{z_2}G^{\phi}(z_1, z_2) \tag{2.17}$$

The similar relation for the Fermi multiplet is

$$\langle\bar{G}(z_1)G(z_2)\rangle = \langle\bar{Q}\bar{\lambda}(z_1)G(z_2)\rangle/\sqrt{2} = \langle\bar{\lambda}(z_1)\bar{Q}G(z_2)\rangle/\sqrt{2} \tag{2.18}$$

$$= \langle\bar{\lambda}(z_1)\left(2\sqrt{2}\partial_z\lambda_- + \frac{\partial E}{\partial\phi_a}\psi_a\right)(z_2)\rangle/\sqrt{2}\,. \tag{2.19}$$

For the case with $E = 0$, we simply get

$$G^{G}(z_1, z_2) = -2\partial_1 G^{\lambda}(z_1, z_2) = 2\partial_2 G^{\lambda}(z_1, z_2)\,. \tag{2.20}$$

The D-terms of a chiral and a Fermi superfields are respectively

$$S^0_{\Phi} = -\int d^2z d\theta^+ d\bar{\theta}^+\bar{\Phi}\partial_{\bar{z}}\Phi\,, \tag{2.21}$$

$$S^0_{\Lambda} = \frac{1}{2}\int d^2z d\theta^+ d\bar{\theta}^+\bar{\Lambda}\Lambda\,. \tag{2.22}$$

In addition, we turn on holomorphic superpotentials that contribute F-term potentials. For the $\mathcal{N} = (0, 2)$ models, the holomorphic superpotential takes a general form

$$\int dx^2 d\theta^+ G(x, \theta^+, \bar{\theta}^+)\,, \tag{2.23}$$

where $G(x, \theta, \bar{\theta})$ is some fermionic superfield that satisfies $\bar{D}_+G = 0$. It is easy to check that the above results agree with the Euclidean continuation of the results [128] in Lorentzian signature.

2.2 The $\mathcal{N} = (0, 2)$ SYK model

We consider a special model of N chiral multiplets and M Fermi multiplets with the F-term potential

$$G(x, \theta, \bar{\theta}) = \frac{J_{ia_1\ldots a_q}}{q!}\Lambda^i_-\Phi^{a_1}\ldots\Phi^{a_q}\,, \tag{2.24}$$

where $i, j, k, \ldots$ label the Fermi multiplets and $a, b, \ldots$ label the chiral multiplets. The $J_{ia_1\ldots a_q}$ coupling has dimension $(\frac{1}{2}, \frac{1}{2})$ and is from a Gaussian distribution

$$\langle J_{ia_1\ldots a_q}J_{ia_1\ldots a_q}\rangle = \frac{(q-1)!}{N^q}J^2\,. \tag{2.25}$$

JHEP12(2018)065

In component form, the above action reads

$$S_{\rm int} = \int d^2x \left(\frac{\sqrt{2}J_{ia_1\ldots a_q}}{(q-1)!}\lambda^i\psi^{a_1}\phi^{a_2}\ldots\phi^{a_q} + \frac{\sqrt{2}J_{ia_1\ldots a_q}}{q!}G^i\phi^{a_1}\ldots\phi^{a_q} + \text{h.c.}\right). \quad (2.26)$$

When $M = N$ the supersymmetry is enhanced to $\mathcal{N} = (2,2)$ and the theory reduces to the models discussed in [101, 112] whose action is recast in (A.3).

The self-energies of the fields are

$$\Sigma^{\psi}(z_1,z_2) = 2J^2\frac{M}{N}G^{\lambda}(z_1,z_2)(G^{\phi}(z_1,z_2))^{q-1}\,, \quad (2.27)$$

$$\Sigma^{\phi}(z_1,z_2) = (q-1)2\frac{M}{N}J^2(G^{\phi}(z_1,z_2))^{q-2}G^{\lambda}(z_1,z_2)G^{\psi}(z_1,z_2) + 2J^2\frac{M}{N}(G^{\phi}(z_1,z_2))^{q-1}G^{G}(z_1,z_2)\,, \quad (2.28)$$

$$\Sigma^{G}(z_1,z_2) = \frac{2J^2}{q}(G^{\phi}(z_1,z_2))^{q}\,, \quad (2.29)$$

$$\Sigma^{\lambda}(z_1,z_2) = 2J^2(G^{\phi}(z_1,z_2))^{q-1}G^{\psi}(z_1,z_2)\,. \quad (2.30)$$

We solve the equation in the $N, M \gg 1$ limit with $\mu = \frac{M}{N}$ a free parameter. It is easy to get the set of $\mathcal{N} = (0,2)$ supersymmetric solutions of the form

$$G_c^I(z_1,z_2) = \frac{n_I}{(z_1-z_2)^{2h_I}(\bar{z}_1-\bar{z}_2)^{2\tilde{h}_I}}\,, \quad (2.31)$$

where $n_\lambda n_\phi^q = -\frac{(q-1)q}{2\pi^2J^2(\mu q^2-1)}$ and

$$h_\phi = \frac{\mu q-1}{2\mu q^2-2}\,,\quad h_\psi = \frac{\mu q^2+\mu q-2}{2\mu q^2-2}\,,\quad h_\lambda = \frac{q-1}{2\mu q^2-2}\,,\quad h_G = \frac{\mu q^2+q-2}{2\mu q^2-2} \quad (2.32)$$

$$\tilde{h}_\phi = \frac{\mu q-1}{2\mu q^2-2}\,,\quad \tilde{h}_\psi = \frac{\mu q-1}{2\mu q^2-2}\,,\quad \tilde{h}_\lambda = \frac{\mu q^2+q-2}{2\mu q^2-2}\,,\quad \tilde{h}_G = \frac{\mu q^2+q-2}{2\mu q^2-2}\,. \quad (2.33)$$

One can solve the Schwinger-Dyson equation numerically to confirm that the model indeed flows to this IR solution. The numerical solution is shown in figure 1.[1]

We should comment on one subtlety in this computation. Since we look for supersymmetric solutions, we only need to solve the Schwinger-Dyson equation of one component of each multiplet; the equation of the other component is then automaticaly satisfied due

[1]Our numerical analysis is done in terms of the superfields that is analogous to [101]. The only difference is that in our case we have a chiral supersymmetry and the model contains a different set of Fermi multiplets. Since the new ingredient — namely the Fermi multiplet — is fermionic, it does not bring new difficulties, such as bosonic zero modes and associated divergences, comparing to the computation in [101]. As a result, our results are obtained straightforwardly: we start from the free field two-point functions of the chiral and Fermi multiplets, and use the two coupled Schwinger-Dyson equations to recursively update the expressions of the two-point functions. This recursive process follows straightforwardly from the method presented in e.g. [6, 101], and we do not repeat here. The results converge to the solution shown in figure 1, where we plots the different components of the superfields explicitly.

JHEP12(2018)065

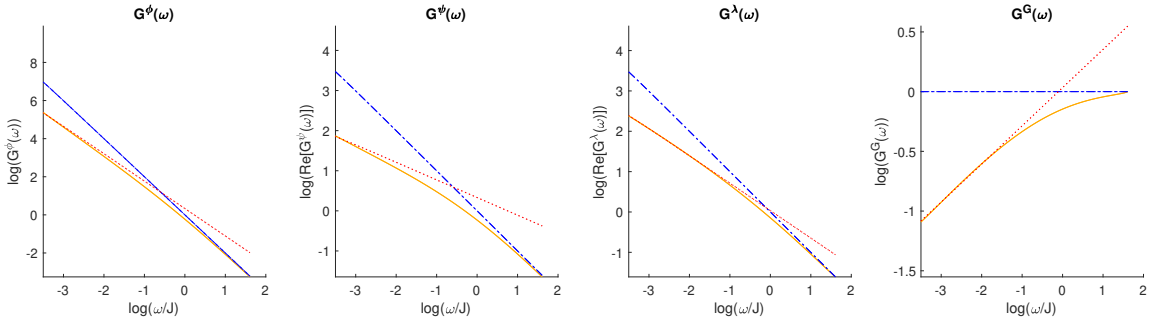

Figure 1. Numerical solutions to the Schwinger-Dyson equations. The blue dash-dot lines are the free propagators in the UV, the red dotted lines are the IR solutions. The yellow curves are result from solving the Schwinger-Dyson equations numerically. One observes that the numerical solutions interpolate between the UV and IR behaviors. The calculation is done for $q = 3$, $\mu = 1.5$.

to supersymmetry. When we solve the equations of the chiral multiplet, we notice that in the UV regime the Fourier transform involves an integral of the form

$$\int r dr d\theta \, r^{2\frac{\mu q-1}{\mu q^2-1}-3} e^{i\theta} e^{irp\cos\theta} \,. \tag{2.34}$$

If we directly count the power of r, it seems that there is a divergence in this Fourier transformation. However, when we check the behavior near $r = 0$, we can expand the $e^{ircos\theta}$ factor to get

$$\int dr d\theta r^{2\frac{\mu q-1}{\mu q^2-1}-2}(1 + irp\cos\theta + \ldots)e^{i\theta} \,. \tag{2.35}$$

We observe that the first term vanishes due to the $e^{i\theta}$ in the θ integral.[2] So the leading term at $r \sim 0$ is

$$\int dr d\theta \, ipr^{2\frac{\mu q-1}{\mu q^2-1}-1} \cos\theta e^{i\theta} \,. \tag{2.36}$$

Therefore as long as we focus on the models with $\mu > \frac{1}{q}$, this integral converges and the model does flow to the IR solution we found above.

3 Four-point functions

In this section, we consider 4-point functions of this model. Because there are two different types of multiplets in the model, there will be a few different 4-point correlation functions. As in the 1-dimensional cases [39, 99, 102], the correlation function can be computed either in terms of superfields or component fields. In the rest of the paper we work in the component formalism.

[2] We thank Douglas Stanford for pointing this out.

JHEP12(2018)065

3.1 Operator spectrum

We are interested in the 4-point function $\langle\bar{\phi}^i\phi^i\bar{\phi}^j\phi^j\rangle$, which mixes with $\langle\bar{\phi}^i\phi^i\bar{\psi}^j\psi^j\rangle$, $\langle\bar{\phi}^i\phi^i\bar{\lambda}^j\lambda^j\rangle$, $\langle\bar{\psi}^i\psi^i\bar{\lambda}^j\lambda^j\rangle$ and $\langle\bar{\phi}^i\phi^i\bar{G}^jG^j\rangle$. There are in total 9 kernels that contribute to these 4-point functions.

The kernels take the following expressions

$$\begin{aligned}K^{\phi\phi}(z_1,z_2,z_3,z_4) &= 2(q-1)J^2\frac{M}{N}G^\phi(z_{13})G^\phi(z_{24})G^G(z_{34})(G^\phi(z_{34}))^{q-2} \\ &\quad + 2(q-1)(q-2)J^2\frac{M}{N}G^\phi(z_{13})G^\phi(z_{24})G^\psi(z_{34})G^\lambda(z_{34})(G^\phi(z_{34}))^{q-3} \qquad (3.1)\\ K^{\phi\psi}(z_1,z_2,z_3,z_4) &= 2(q-1)J^2\frac{M}{N}G^\phi(z_{13})G^\phi(z_{24})G^\lambda(z_{34})(G^\phi(z_{34}))^{q-2} \qquad (3.2)\\ K^{\phi\lambda}(z_1,z_2,z_3,z_4) &= 2(q-1)J^2G^\phi(z_{13})G^\phi(z_{24})G^\psi(z_{34})(G^\phi(z_{34}))^{q-2} \qquad (3.3)\\ K^{\phi G}(z_1,z_2,z_3,z_4) &= 2J^2G^\phi(z_{13})G^\phi(z_{24})(G^\phi(z_{34}))^{q-1} \qquad (3.4)\\ K^{\psi\phi}(z_1,z_2,z_3,z_4) &= -2(q-1)J^2\frac{M}{N}G^\psi(z_{13})G^\psi(z_{24})G^\lambda(z_{34})(G^\phi(z_{34}))^{q-2} \qquad (3.5)\\ K^{\psi\lambda}(z_1,z_2,z_3,z_4) &= -2J^2G^\psi(z_{13})G^\psi(z_{24})(G^\phi(z_{34}))^{q-1} \qquad (3.6)\\ K^{\lambda\phi}(z_1,z_2,z_3,z_4) &= -2(q-1)J^2\frac{M}{N}G^\lambda(z_{13})G^\lambda(z_{34})G^\psi(z_{34})(G^\phi(z_{34}))^{q-2} \qquad (3.7)\\ K^{\lambda\psi}(z_1,z_2,z_3,z_4) &= -2J^2\frac{M}{N}G^\lambda(z_{13})G^\lambda(z_{24})(G^\phi(z_{34}))^{q-1} \qquad (3.8)\\ K^{G\phi}(z_1,z_2,z_3,z_4) &= -2J^2\frac{M}{N}G^G(z_{13})G^G(z_{24})(G^\phi(z_{34}))^{q-1}\,, \qquad (3.9)\end{aligned}$$

where we use the short hand notation $z_{ij}=z_i-z_j$. The following ansatz

$$\Phi^I(z_1,z_2)=(z_{12})^{h-2h_I}(\bar{z}_{12})^{\tilde{h}-2\tilde{h}_I}\,,\qquad I=\phi,\psi,\lambda,G\,, \qquad (3.10)$$

turns out to be the eigenfunctions of the above kernels

$$K^{(IJ)}*\Phi^J=k^{IJ}\Phi^I\,, \qquad (3.11)$$

where the $*$ denotes a convolution in position space. Making use of the following integral formula [101]

$$\begin{aligned}&\int d^2y(y-t_0)^{a+n}(\bar{y}-\bar{t}_0)^a(t_1-y)^{b+m}(\bar{t}_1-\bar{y})^b\\ &=(t_0-t_1)^{a+n+b+m+1}(\bar{t}_0-\bar{t}_1)^{a+b+1}\pi\frac{\Gamma(a+1)\Gamma(b+1)\Gamma(-a-b-m-n-1)}{\Gamma(a+b+2)\Gamma(-a-n)\Gamma(-b-m)}\,, \qquad (3.12)\end{aligned}$$

one finds the non-vanishing eigenvalues to be

$$k^{\phi\phi}=\frac{\mu(q-1)^2q\left(\mu q^2-2\mu q+1\right)\Gamma\left(1-2h_\phi\right)^2\Gamma\left(2h_\phi-h\right)\Gamma\left(\tilde{h}-1+2h_\phi\right)}{\left(\mu q^2-1\right)^2\Gamma\left(2h_\phi\right)^2\Gamma\left(2-2h_\phi-h\right)\Gamma\left(\tilde{h}+1-2h_\phi\right)} \qquad (3.13)$$

$$k^{\phi\psi}=-\frac{\mu(q-1)^2q\Gamma\left(1-2h_\phi\right)^2\Gamma\left(2h_\phi-h\right)\Gamma\left(\tilde{h}-1+2h_\phi\right)}{2\left(\mu q^2-1\right)\Gamma\left(2h_\phi\right)^2\Gamma\left(2-2h_\phi-h\right)\Gamma\left(\tilde{h}+1-2h_\phi\right)} \qquad (3.14)$$

JHEP12(2018)065

$$k^{\phi\lambda} = -\frac{4\pi^2 J^2 (q-1) n_\phi^{q+1} (\mu q - 1) \Gamma\left(1-2h_\phi\right)^2 \Gamma\left(2h_\phi - h\right) \Gamma\left(\tilde{h} - 1 + 2h_\phi\right)}{\left(\mu q^2 - 1\right) \Gamma\left(2h_\phi\right)^2 \Gamma\left(2 - 2h_\phi - h\right) \Gamma\left(\tilde{h} + 1 - 2h_\phi\right)} \tag{3.15}$$

$$k^{\phi G} = \frac{2\pi^2 J^2 n_\phi^{q+1} \Gamma\left(1-2h_\phi\right)^2 \Gamma\left(2h_\phi - h\right) \Gamma\left(\tilde{h} - 1 + 2h_\phi\right)}{\Gamma\left(2h_\phi\right)^2 \Gamma\left(2 - 2h_\phi - h\right) \Gamma\left(\tilde{h} + 1 - 2h_\phi\right)} \tag{3.16}$$

$$k^{\psi\phi} = -\frac{2\mu (q-1)^2 q (\mu q - 1)^2 \Gamma\left(1-2h_\phi\right)^2 \Gamma\left(1 + 2h_\phi - h\right) \Gamma\left(\tilde{h} - 1 + 2h_\phi\right)}{\left(\mu q^2 - 1\right)^3 \Gamma\left(1 + 2h_\phi\right)^2 \Gamma\left(1 - 2h_\phi - h\right) \Gamma\left(\tilde{h} + 1 - 2h_\phi\right)} \tag{3.17}$$

$$k^{\psi\lambda} = \frac{8\pi^2 J^2 n_\phi^{q+1} (\mu q - 1)^2 \Gamma\left(1-2h_\phi\right)^2 \Gamma\left(1 + 2h_\phi - h\right) \Gamma\left(\tilde{h} - 1 + 2h_\phi\right)}{\left(\mu q^2 - 1\right)^2 \Gamma\left(1 + 2h_\phi\right)^2 \Gamma\left(1 - 2h_\phi - h\right) \Gamma\left(\tilde{h} + 1 - 2h_\phi\right)} \tag{3.18}$$

$$k^{\lambda\phi} = -\frac{\mu (q-1)^3 q^2 n_\phi^{-q-1} (\mu q - 1) \Gamma\left(-2h_\lambda\right)^2 \Gamma\left(2h_\lambda - h\right) \Gamma\left(2h_\lambda + \tilde{h}\right)}{4\pi^2 J^2 \left(\mu q^2 - 1\right)^3 \Gamma\left(2h_\lambda\right)^2 \Gamma\left(2 - h - 2h_\lambda\right) \Gamma\left(\tilde{h} - 2h_\lambda\right)} \tag{3.19}$$

$$k^{\lambda\psi} = \frac{\mu (q-1)^2 q^2 n_\phi^{-q-1} \Gamma\left(-2h_\lambda\right)^2 \Gamma\left(2h_\lambda - h\right) \Gamma\left(2h_\lambda + \tilde{h}\right)}{8\pi^2 J^2 \left(\mu q^2 - 1\right)^2 \Gamma\left(2h_\lambda\right)^2 \Gamma\left(2 - h - 2h_\lambda\right) \Gamma\left(\tilde{h} - 2h_\lambda\right)} \tag{3.20}$$

$$k^{G\phi} = \frac{\mu (q-1)^4 q^2 n_\phi^{-q-1} \Gamma\left(-2h_\lambda\right)^2 \Gamma\left(1 - h + 2h_\lambda\right) \Gamma\left(2h_\lambda + \tilde{h}\right)}{2\pi^2 J^2 \left(\mu q^2 - 1\right)^4 \Gamma\left(1 + 2h_\lambda\right)^2 \Gamma\left(1 - h - 2h_\lambda\right) \Gamma\left(\tilde{h} - 2h_\lambda\right)} \,. \tag{3.21}$$

It is convenient to organize the eigenvalues into an 8×8 matrix

$$\begin{pmatrix} 0 & 1 \\ 1 & 0 \end{pmatrix} \otimes \begin{pmatrix} k^{\phi\phi} & k^{\phi\psi} & k^{\phi\lambda} & k^{\phi G} \\ k^{\psi\phi} & 0 & k^{\psi\lambda} & 0 \\ k^{\lambda\phi} & k^{\lambda\psi} & 0 & 0 \\ k^{G\phi} & 0 & 0 & 0 \end{pmatrix} \tag{3.22}$$

and the final eigenvalues come from diagonalizing this matrix. Here the presence of the extra $\sigma_1 = \begin{pmatrix} 0 & 1 \\ 1 & 0 \end{pmatrix}$ matrix is due to the form of the interaction in (2.26). To illustrate it, we consider, for example, the action of the kernel $K^{\phi\psi}$ on the eigenfunction Φ^ψ. As shown in figure 2, after the action of the kernel, the upper leg becomes a conjugate field, namely the direction of the arrow is flipped. Therefore the actual eigenfunctions come in conjugate pairs. This means the actual action of the kernel should be like in figure 3. Further notice that due to the form of the IR propagators, the two entries in the kernel matrix share the same expression. This leads to the extra tensor product with the σ_1 matrix in (3.22).

Diagonalizing this matrix, there are 4 eigenvalues being the 4 roots of the following equation

$$\begin{aligned} E_c(x, h, \tilde{h}, \mu, q) = {} & x^4 - k^{\phi\phi} x^3 - \left(k^{\phi G} k^{G\phi} + k^{\phi\psi} k^{\psi\phi} + k^{\phi\lambda} k^{\lambda\phi} + k^{\psi\lambda} k^{\lambda\psi}\right) x^2 \\ & + \left(k^{\phi\phi} k^{\psi\lambda} k^{\lambda\psi} - k^{\phi\psi} k^{\psi\lambda} k^{\lambda\phi} - k^{\phi\lambda} k^{\psi\phi} k^{\lambda\psi}\right) x + k^{\phi G} k^{\psi\lambda} k^{\lambda\psi} k^{G\phi} \\ = {} & 0 \,, \end{aligned} \tag{3.23}$$

JHEP12(2018)065

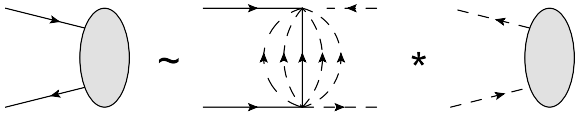

Figure 2. Action of a single kernel.

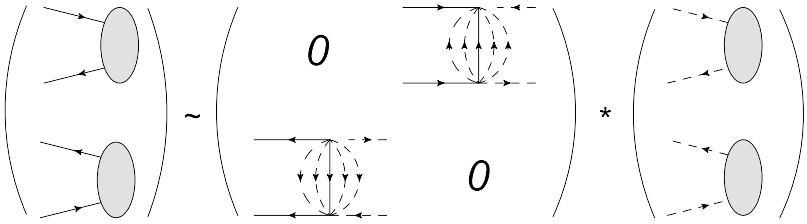

Figure 3. The eigenfunctions come in pairs. The two kernels in the 2×2 matrix give identical contributions to the eigenvalue matrix (3.22), which leads to the extra σ_1 factor.

which we will call the symmetric eigenvalues. There are another 4 eigenvalues being the solution of the equation

$$\begin{aligned} E_c'(x,h,\tilde{h},\mu,q) &= x^4 + k^{\phi\phi}x^3 - \left(k^{\phi G}k^{G\phi} + k^{\phi\psi}k^{\psi\phi} + k^{\phi\lambda}k^{\lambda\phi} + k^{\psi\lambda}k^{\lambda\psi}\right)x^2 \\ &\quad - \left(k^{\phi\phi}k^{\psi\lambda}k^{\lambda\psi} - k^{\phi\psi}k^{\psi\lambda}k^{\lambda\phi} - k^{\phi\lambda}k^{\psi\phi}k^{\lambda\psi}\right)x + k^{\phi G}k^{\psi\lambda}k^{\lambda\psi}k^{G\phi} \\ &= 0\,, \end{aligned} \tag{3.24}$$

which we will call the antisymmetric eigenvalues. Their presence is a result of the complex fundamental fields in our model (2.26), similar to the 1-dimensional cases [99, 102, 127]. We have not succeeded in getting simple expressions of the eigenvalues. But the equation (3.23) and (3.24) pass a few consistency checks.

First, as we discussed above we expect the result to reduce to that of the $\mathcal{N} = (2,2)$ model in the $\mu \to 1$ limit. Indeed, we can solve (3.23) and (3.24) at $\mu = 1$ to find the following 8 eigenvalues

$$\begin{aligned} &\pm k^{FB}\left(h - \frac{1}{2}, \tilde{h} - 1\right)\,, \quad \pm k^{FB}\left(h + \frac{1}{2}, \tilde{h} - 1\right)\,, \\ &\pm k^{FB}\left(h - \frac{1}{2}, \tilde{h}\right)\,, \qquad \pm k^{FB}\left(h + \frac{1}{2}, \tilde{h}\right)\,, \end{aligned} \tag{3.25}$$

which are consistent with the $\mathcal{N} = (2,2)$ result. At generic μ, the eigenfunctions can be considered as deformations of the eigenvalues (3.25).

Another consistency check is the presence of the stress-energy tensor at any generic μ. To see this, recall that in this model the 4-point functions are sums of ladder diagrams. Therefore there is always a factor

$$\frac{1}{1 - k_i}\,, \tag{3.26}$$

where $i = 1, \ldots, 8$ are the 8 eigenvalues obtained from solving (3.23) and (3.24). Then an operators with dimension $(h_*, \tilde{h}_*)$ running in each channel can be represented by a pole

JHEP12(2018)065

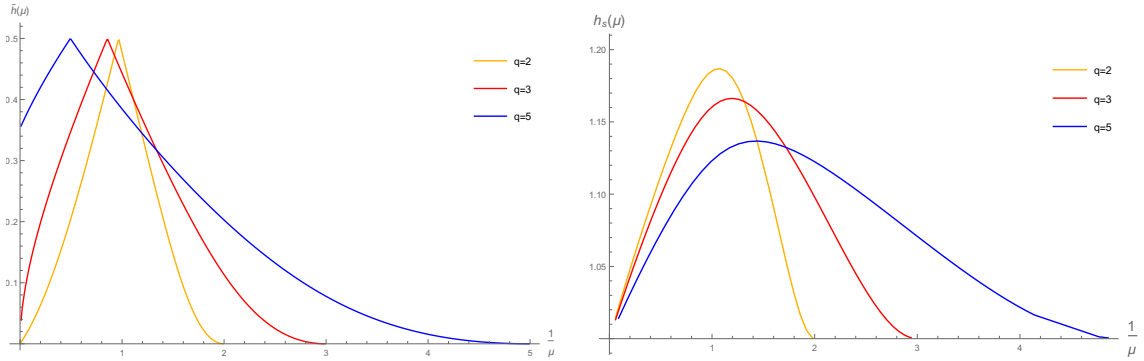

(a) The symmetric channel. **(b)** The antisymetric channel.

Figure 4. The lowest dimensions of the scalar operators in the four point function. The plots illustrate how does the dimension change as a function of μ. The kinks on each curve in figure 4a is the crossover point of the operator and its "shadow" operator due to the symmetry $h \leftrightarrow 1-h$ and $\tilde{h} \leftrightarrow 1-\tilde{h}$.

in the factor (3.26) at $(h, \tilde{h}) = (h_*, \tilde{h}_*)$. For the special case of the stress-energy tensor, we simply expand the coefficients of (3.23) and (3.24) to the first order of $h-2$ and then find the eigenvalues to the first order of $h-2$. It turns out that there is always a solution behaves like

$$k^1 = 1 + \frac{\left(\mu q^2 - 1\right)^2}{q\left(\mu^2 q^2 - 1\right)}(h-2) + \mathcal{O}\left((h-2)^2\right) , \tag{3.27}$$

which corresponds to the deformation of $k^{FB}(h-\frac{1}{2}, \tilde{h})$. Therefore $(h, \tilde{h}) = (2, 0)$ is always a solution that sets some eigenvalue to 1. This can also be confirmed by explicitly verifying that $E(1, 2, 0, \mu, q) = 0$.

To get the complete spectrum of the operators in the IR limit of the model, we need to find their corresponding $(h, \tilde{h})$ that makes some eigenvalues to 1. Therefore the dimension of the operators should solve

$$E_c(1, h_s, \tilde{h}_s, \mu, q) = 0\,, \qquad E_c'(1, h_a, \tilde{h}_a, \mu, q) = E_c(-1, h_a, \tilde{h}_a, \mu, q) = 0\,, \tag{3.28}$$

where we use the subscript a, s to present operators in the symmetry and antisymmetric channels.

For instance, we get the lowest dimensions of scalar operators running in the 4-point functions of the fundamental fields by solving

$$E_c(1, h_s, h_s, \mu, q) = 0\,, \qquad E_c(-1, h_a, h_a, \mu, q) = 0\,, \tag{3.29}$$

for generic μ and q. The equations are easily solved numerically. The solutions to the equation $E_c(\pm 1, h_s, h_s, \mu, q) = 0$ is shown in figure 4. As we can see the dimension of the scalar operators in the symmetric channel approach zero as the μ approaches $\frac{1}{q}$. In addition, the dimension of the operators in the antisymmetric channel is larger than those in the symmetric channel. This is as expected since the operators in the antisymmetric channel involves one more derivative.

JHEP12(2018)065

We also computed other 4-point functions where fermionic operators runs in the ladder. The details are elaborated in appendix . We only outline here that one can check explicitly that at the $\mu = 1$ point, we do observe both $(h, \tilde{h}) = (\frac{3}{2}, 0)$ and $(h, \tilde{h}) = (0, \frac{3}{2})$ operators that correspond to the supercharges in the holomorphic and antiholomorphic sectors. This again confirms that at $\mu = 1$ our model has an enhanced $\mathcal{N} = (2, 2)$ supersymmetry. We further check that as long as $\mu \neq 1$ the left-moving supercharges are lifted and stop generating supersymetry in the left-moving sector. This is as we expected since the model only has $\mathcal{N} = (0, 2)$ supersymmetry at generic μ.

3.2 Chaotic behavior

One can further go to the chaos region and study the out-of-time-ordered correlators. For this we simply consider retarded kernels. We start from the Euclidean propagators on a periodic τ direction and a noncompact spatial direction x

$$G^I_{th}(\tau_1, x_1, \tau_2, x_2) = \frac{n_I}{\left(2\sinh(\frac{x_{12}+i\tau_{12}}{2})\right)^{2h_I}\left(2\sinh(\frac{x_{12}-i\tau_{12}}{2})\right)^{2\tilde{h}_I}}\,. \tag{3.30}$$

The retarded propagators can be computed from analytic continuation of (3.30)

$$G^b_R(t_1, x_1, t_2, x_2) = -\frac{2i\sin\left(\pi(h_b+\tilde{h}_b)\right)\theta(t_{12}-|x_{12}|)n_b}{\left(2\sinh\left(\frac{t_{12}-x_{12}}{2}\right)\right)^{2h_b}\left(2\sinh\left(\frac{t_{12}+x_{12}}{2}\right)\right)^{2\tilde{h}_b}}\,, \qquad b = \phi, G \tag{3.31}$$

$$G^f_R(t_1, x_1, t_2, x_2) = \frac{2\cos\left(\pi(h_f+\tilde{h}_f)\right)\theta(t_{12}-|x_{12}|)n_f}{\left(2\sinh\left(\frac{t_{12}-x_{12}}{2}\right)\right)^{2h_f}\left(2\sinh\left(\frac{t_{12}+x_{12}}{2}\right)\right)^{2\tilde{h}_f}}\,, \qquad f = \psi, \lambda\,. \tag{3.32}$$

We also need the set of ladder rung propagators between the rails. They can be obtained from a simple analytic continuation

$$\begin{aligned} G^I_{lr}(t_1, x_1; t_2, x_2) &= G_{th}(it_1, x_1; it_2 + \pi, x_2) \\ &= \frac{n_I}{\left(2\cosh(\frac{x_{12}-t_{12}}{2})\right)^{2h_I}\left(2\cosh(\frac{x_{12}+t_{12}}{2})\right)^{2\tilde{h}_I}} \end{aligned} \tag{3.33}$$

The set of retarded kernels can be obtained from (3.13)–(3.21) by replacing the propagators on the rails by the corresponding retarded ones (3.31) or (3.32) and replacing the ladder rung propagators by the ones in (3.33).

Following [101], we introduce the new variable

$$u = e^{x-t}\,, \qquad v = e^{-x-t}\,, \tag{3.34}$$

for the retarded propagators on the upper rail and

$$u = -e^{x-t}\,, \qquad v = -e^{-x-t}\,, \tag{3.35}$$

for the retarded propagators on the lower rail. We consider the following ansatz

$$\Psi^I_R(3, 4) = (-u_3u_4)^{\frac{h_3+h_4}{2}}(-v_3v_4)^{\frac{\tilde{h}_3+\tilde{h}_4}{2}}u_{34}^{h-h_3-h_4}v_{34}^{\tilde{h}-\tilde{h}_3-\tilde{h}_4}\,, \tag{3.36}$$

JHEP12(2018)065

where h_i, $\tilde{h}_i$ labels the dimensions of the operators at t_i, x_i. In terms of the t and x coordinate, (3.36) becomes

$$\Psi_R^I(1,2) = \frac{e^{-\frac{1}{2}(h+\tilde{h})(t_1+t_2)-\frac{1}{2}(h-\tilde{h})(x_1+x_2)}}{(2\cosh\frac{x_{12}-t_{12}}{2})^{h_1+h_2-h}(2\cosh\frac{x_{12}+t_{12}}{2})^{\tilde{h}_1+\tilde{h}_2-\tilde{h}}}\,. \tag{3.37}$$

Our goal is to find eigenfunctions that grows exponentially with time but remain normalizable in the spatial direction. This requires $h-\tilde{h}$ to be imaginary and we can follow [101] to reparametrize h and $\tilde{h}$ as

$$h = -\frac{\lambda_L}{2} + i\frac{p}{2} \qquad \tilde{h} = -\frac{\lambda_L}{2} - i\frac{p}{2}\,. \tag{3.38}$$

Finding the largest chaotic behavior then means to find the largest λ_L that renders at least one eigenvalues to 1.

As in the case discussed in [101], the convolution integral in the eigenequation

$$K_R^{(ij)} * \Psi_R^j = k_R^{ij}\Psi_R^i\,, \tag{3.39}$$

factorizes into two 1-dimensional integrals in the u, v variables with the eigenfunction (3.36), each of which can be carried out straightforwardly. The resulting eigenvalues are

$$k_R^{\phi\phi} = \frac{2\mu(q-1)^2 q\left(\mu q^2-2\mu q+1\right)\Gamma\left(1-2h_\phi\right)^4\sin^2\left(2\pi h_\phi\right)}{\pi^4\left(\mu q^2-1\right)^2} \tag{3.40}$$

$$\times\sin\left(\frac{\pi}{2}(h+2h_\phi)\right)\Gamma\left(h-1+2h_\phi\right)\Gamma\left(2h_\phi-h\right) \tag{3.41}$$

$$\times\sin\left(\frac{\pi}{2}(\tilde{h}+2h_\phi)\right)\Gamma\left(\tilde{h}-1+2h_\phi\right)\Gamma\left(2h_\phi-\tilde{h}\right) \tag{3.42}$$

$$\times\left(\cos\left(\frac{1}{2}\pi\left(h+\tilde{h}+4h_\phi\right)\right)+\cos\left(\frac{1}{2}\pi(h-\tilde{h})\right)\right) \tag{3.43}$$

$$k_R^{\phi\psi} = \frac{\mu q^2-1}{2\mu q^2-4\mu q+2}k_R^{\phi\phi} \tag{3.44}$$

$$k_R^{\phi\lambda} = \frac{4\pi^2J^2n_\phi^{q+1}(\mu q-1)\left(\mu q^2-1\right)}{\mu(q-1)q\left(\mu q^2-2\mu q+1\right)}k_R^{\phi\phi} \tag{3.45}$$

$$k_R^{\phi G} = \frac{2\pi^2J^2n_\phi^{q+1}\left(\mu q^2-1\right)^2}{\mu(q-1)^2q\left(\mu q^2-2\mu q+1\right)}k_R^{\phi\phi} \tag{3.46}$$

$$k_R^{\psi\phi} = 2\left(h-2h_\phi\right)\frac{\left(h\left(\mu q^2-1\right)-\mu(q-1)q\right)\tan\left(\frac{\pi}{2}(h+2h_\phi)\right)}{\left(\mu q^2-2\mu q+1\right)\tan\left(\frac{\pi}{2}(h+2h_\phi)\right)}k_R^{\phi\phi} \tag{3.47}$$

$$k_R^{\psi\lambda} = \frac{8\pi^2J^2n_\phi^{q+1}(\mu q^2-1)^2\left(h-2h_\phi\right)\left(h-1+2h_\phi\right)\tan\left(\frac{1}{2}\pi\left(h+2h_\phi\right)\right)}{\mu q(q-1)^2\left(\mu q^2-2\mu q+1\right)\tan\left(\frac{\pi}{2}(h+2h_\phi)\right)}k_R^{\phi\phi} \tag{3.48}$$

$$k_R^{\lambda\phi} = -\frac{\mu(q-1)^5q^2(\mu q-1)\sin^2\left(\pi(1+2h_\lambda)\right)}{\pi^6n_\phi^{q+1}J^2\left(\mu q^2-1\right)^5}\Gamma\left(-2h_\lambda\right)^4 \tag{3.49}$$

$$\times\sin\left(\frac{\pi}{2}(h+2h_\lambda)\right)\cos\left(\frac{\pi}{2}(h+2h_\lambda)\right)\Gamma\left(2h_\lambda-h\right)\Gamma\left(h+2h_\lambda-1\right) \tag{3.50}$$

$$\times\sin\left(\frac{\pi}{2}(\tilde{h}+2h_\lambda)\right)\cos\left(\frac{\pi}{2}(\tilde{h}+2h_\lambda)\right)\Gamma\left(\tilde{h}+2h_\lambda\right)\Gamma\left(1+2h_\lambda-\tilde{h}\right) \tag{3.51}$$

JHEP12(2018)065

$$k_R^{\lambda\psi} = \frac{\mu q^2 - 1}{2(q-1)(\mu q - 1)} k_R^{\lambda\phi} \tag{3.52}$$

$$k_R^{g\phi} = -\frac{2\,(h-2h_\lambda)\,(h-1+2h_\lambda)\tan\left(\frac{\pi}{2}(h+2h_\lambda)\right)\tan\left(\frac{\pi h}{2}-1+2h_\lambda\right)}{(q-1)(\mu q-1)\,(\mu q^2-1)^{-1}} k_R^{\lambda\phi}\,. \tag{3.53}$$

In principle, we diagonalize the matrix of retarded kernels, which is the retarded version of (3.22), to get the equation of the eigenvalues

$$\begin{aligned} E_R(x,h,\tilde{h},\mu,q) &= x^4 - k_R^{\phi\phi}x^3 - \left(k_R^{\phi G}k_R^{G\phi} + k_R^{\phi\psi}k_R^{\psi\phi} + k_R^{\phi\lambda}k_R^{\lambda\phi} + k_R^{\psi\lambda}k_R^{\lambda\psi}\right)x^2 \\ &\quad + \left(k_R^{\phi\phi}k_R^{\psi\lambda}k_R^{\lambda\psi} - k_R^{\phi\psi}k_R^{\psi\lambda}k_R^{\lambda\phi} - k_R^{\phi\lambda}k_R^{\psi\phi}k_R^{\lambda\psi}\right)x + k_R^{\phi G}k_R^{\psi\lambda}k_R^{\lambda\psi}k_R^{G\phi} \\ &= 0\,. \end{aligned} \tag{3.54}$$

Then we solve for the h and $\tilde{h}$ that set the eigenvalue to 1. In our case we do not get a simple expression of the eigenfunctions. But we can still find the maximal values of λ_L by a direct analysis of the eigenfunction equation: since we are interested in eigenvalue 1, we can simply set $x = 1$ of the equation (3.54) that determines λ_L as an implicit function of μ and p. We can then find the largest value of λ_L by tuning μ and p.

To proceed we start with a sanity check by focusing on the $\mu = 1$ case and check if the result agrees with the $\mathcal{N} = (2,2)$ result. There are two ways to do such a check. The first approach is noticing that at $\mu = 1$ we can solve the retarded eigenequation (3.54) directly to find that there are 4 eigenvalues

$$k_1^{\mu=1} = -\frac{\Gamma\left(\frac{q}{q+1}\right)^2\Gamma\left(\frac{1}{q+1}-h\right)\Gamma\left(\frac{1}{q+1}-\tilde{h}\right)}{\Gamma\left(\frac{1}{q+1}-1\right)\Gamma\left(1+\frac{1}{q+1}\right)\Gamma\left(\frac{q}{q+1}-h\right)\Gamma\left(\frac{q}{q+1}-\tilde{h}\right)} \tag{3.55}$$

$$k_2^{\mu=1} = -\frac{hq+h-1}{hq+h-q}k_1^{\mu=1} \tag{3.56}$$

$$k_3^{\mu=1} = -\frac{\tilde{h}q+\tilde{h}-1}{\tilde{h}q+\tilde{h}-q}k_1^{\mu=1} \tag{3.57}$$

$$k_4^{\mu=1} = \frac{(hq+h-1)(\tilde{h}q+\tilde{h}-1)}{(hq+h-q)(\tilde{h}q+\tilde{h}-q)}k_1^{\mu=1}\,, \tag{3.58}$$

and indeed $k_1^{\mu=1}$ is identical to the k_R^{BB} function in [101]. Notice that the other $k_i^{\mu=1}$ are due to the super-descendents of the eigenfunction corresponding to $k_1^{\mu=1}$. Hence they are not expected to be related to the k_R^{BF}, k_R^{FB}, k_R^{FF} functions in [101] that are due to different primaries of the third operators in the eigenfunctions.

The second approach is to follow the method we discribed above, namely plug $x = 1$ into the equation (3.54), then setting $\mu = 1$ and looking for maximal λ_L by tuning p. We indeed find a miximal $\lambda_L = 0.5824$ at $p = 0$. This agrees with the result in [101] and confirms the validity of our procedure.

We now move to general μ. Because the integral (3.39) again factorize into two 1-dimensional ones, by a similar monotonic argument as in [101] we expect the largest λ_L is reached at $p = 0$. This is indeed true as one can check explicitly. We present the p

JHEP12(2018)065

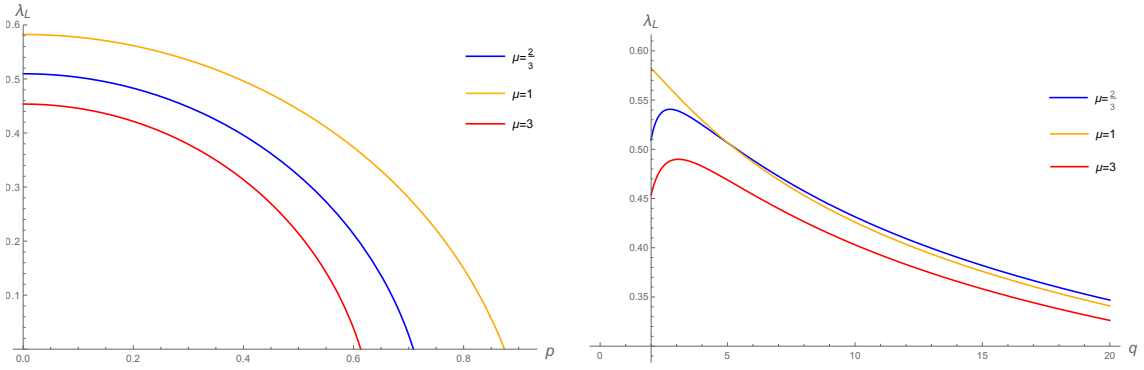

(a) p dependence. **(b)** q dependence.

Figure 5. Functional dependence of the Lyapunov exponent λ_L.

dependence for some special values of μ in figure 5a. It is also straightforward to check the q dependence of λ_L, a few examples of which are presented in figure 5b. We find the largest λ_L appears close to the smallest q that leads to nontrivial interactions, namely $q = 2$.

Then we look for maximal λ_L as a function of μ. The general dependence is shown in figure 6. One finds a maximum of λ_L as we change μ. Interestingly, this maximal value does not appear at the special point $\mu = 1$; rather it appears at $\mu \simeq 0.9802$ where the maximal value is $\lambda_L(p = 0, \mu = 0.9802) = 0.5825$. This maximal value is only slightly larger than the value for the $\mathcal{N} = (1, 1)$ and $\mathcal{N} = (2, 2)$ model where $\lambda_L(p = 0, \mu = 1) \simeq 0.5824$. Notice that in determining this Lyapunov exponent we do all the computation analytically, except for the very last step where we find the solution to a given equation numerically. Since the error of this last step is very well controlled, our result is genuinely different from the exponent in the $\mathcal{N} = (1, 1)$ or $\mathcal{N} = (2, 2)$ model.

It is not clear what is the physical reason of why the maximal value of λ_L in the class of models we consider here is only slightly higher than that found in the special case $\mu = 1$, and why the correspnding μ is only slightly smaller than 1. The slightly larger Lyapunov exponent probably indicates that there should be a wider class of similar models that are continuously related. Our model, and the $\mathcal{N} = (1, 1)$, $\mathcal{N} = (2, 2)$ models are only examples that sit on a generic point on the moduli space. It is conceivable that there are special theories on (some corners) the moduli space that have larger, or even maximal, Lyapunov exponent.

4 Two higher-spin limits

It is widely believed that the SYK-like models have close relations with higher-spin theories; higher-spin theories should be thought as a subsector of some tensionless limit of string theory, while the SYK model should be holographically dual to some string theory with finite tension [6]. Therefore it is tempting to find a direct relation between SYK-like models and models with higher-spin symmetry. In 1-dimension, one example of such relation is discussed in [39]. In this section we give another explicit example of such connection in 2 dimension. The basic idea is to tune the free parameter to some critical/singular value

JHEP12(2018)065

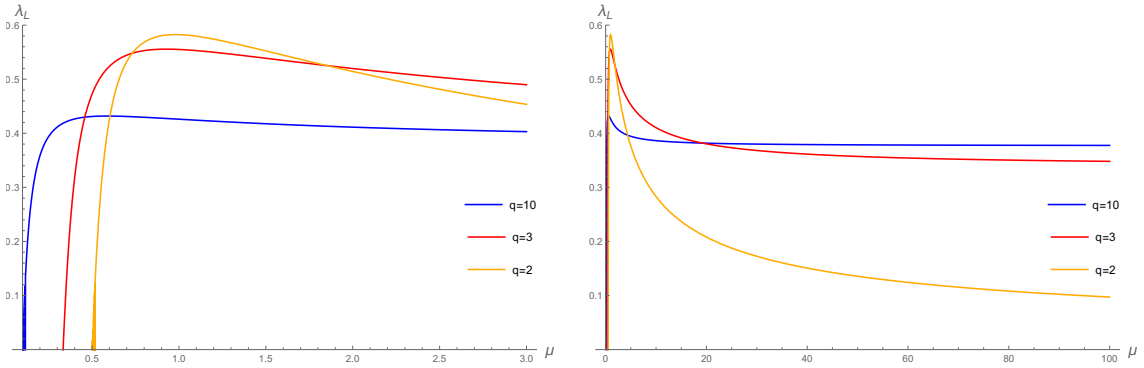

(a) Small μ region. **(b)** Large μ region.

Figure 6. μ dependence of the Lyapunov exponent λ_L. The yellow, red and blue curves are evaluated at $p = 0$ and $q = 2$, 3, 10 respectively.

where the model develops some properties that is characteristic for models with higher-spin symmetry. In particular, we find two singular limits at the two ends of the range of μ, where the model (2.26) develops emergent higher-spin symmetries. In the following we discuss the two limits separately.

4.1 The $\mu q \to 1^+$ ("classical chiral") limit

The Fourier transform (2.36) at the special value $\mu = \frac{1}{q}$ has a logarithmic divergence. This means a proper renormalization analysis of the model at $\mu = \frac{1}{q}$ is needed. We will not do it here and will postpone this in future work. Nevertheless, we consider the limit

$$\mu \to \left(\frac{1}{q}\right)^+ . \tag{4.1}$$

Taking the limit in this manner, all our previous computation are valid since there is no divergence in the limiting process. The IR dimensions of the various fields in this limit are

$$\lim_{\mu\to(1/q)^+} h_\phi = 0\,, \qquad \lim_{\mu\to(1/q)^+} h_\psi = \frac{1}{2}\,, \qquad \lim_{\mu\to(1/q)^+} h_\lambda = \frac{1}{2}\,, \qquad \lim_{\mu\to(1/q)^+} h_G = 1 \tag{4.2}$$

$$\lim_{\mu\to(1/q)^+} \tilde{h}_\phi = 0\,, \qquad \lim_{\mu\to(1/q)^+} \tilde{h}_\psi = 0\,, \qquad \lim_{\mu\to(1/q)^+} \tilde{h}_\lambda = 1\,, \qquad \lim_{\mu\to(1/q)^+} \tilde{h}_G = 1\,, \tag{4.3}$$

where the dimension of the ϕ and ψ fields take the values in a free chiral multiplet. This is a first hind that we should expect a larger higher spin type symmetry to emerge in this limit. This is consistent with the result from the chaos analysis in the previous section; as shown in figure 6 the Lyapunov exponents all vanish as $\mu \to \left(\frac{1}{q}\right)^+$ for any $q > 1$. In the following we confirm the existence of a higher-spin symmetry from a few different aspects.

A tower of conserved higher-spin operators. Given the above motivation, we look for a tower of higher-spin operators in the limit (4.1). Recall that in 2 dimensions, conserved higher-spin operators are represented by (anti-)holomorphic primary operators with vanishing (right) left conformal dimensions. Therefore we extend the computation in the

JHEP12(2018)065

	holomorphic operators	anti-holomorphic operators
symmetric channel	$(h,\tilde{h})=(s,0),\ s\geq 1$	$(h,\tilde{h})=(0,s),\ s\geq 1$
antisymmetric channel	$(h,\tilde{h})=(s,0),\ s\geq 1$	$(h,\tilde{h})=(0,s),\ s\geq 1$

Table 1. The conserved operators in the limit (4.1).

previous subsection to find such (anti-)holomorphic primary operators in the limit (4.1). For this we go back to (3.28) and look for solutions of

$$\lim_{\mu\to(1/q)^+} E_c(1,\tilde{h}+s,\tilde{h},\mu,q)=0\,,\qquad \lim_{\mu\to(1/q)^+} E_c(-1,\tilde{h}+s,\tilde{h},\mu,q)=0\,,\quad s>0\,,\ \tilde{h}\to 0\,, \tag{4.4}$$

that correspond to the holomorphic higher-spin operators in the symmetric and antisymmetric channel. Because our model has a manifest $\mathcal{N}=(0,2)$ supersymmetry, the operator spectrum of the holomorphic and anti-holomorphic operators could be different. Therefore we need to find the spectrum of the anti-holomorphic operators seperately, which corresponds to solving

$$\lim_{\mu\to(1/q)^+} E_c(1,h,h+s,\mu,q)=0\,,\qquad \lim_{\mu\to(1/q)^+} E_c(-1,h,h+s,\mu,q)=0\,,\quad s>0\,,\ h\to 0\,. \tag{4.5}$$

Furthermore, the operators running in the channel tha is detected by our ladder diagrams (3.1)–(3.9) are all bosonic, so we only look for solutions with integer s, at any q. The equations are again easily solved numerically, and we get a function $\tilde{h}(\mu)$ or $h(\mu)$ of any given s and q. We summarize the operators that become (anti)-holomorphic in the limit (4.1) in table 1. Some example solutions of (4.4) and (4.5) near the limit (4.1) are illustrated in figure 7. From this result we indeed observe that in the $\mu\to\left(\frac{1}{q}\right)^+$ limit the dimensions of some operators in 4-point functions approaches the dimensions of the (anti-)holomorphic higher-spin operators shown in the above table. This result indicates that a tower of conserved higher spin currents emerges in the limit (4.1).

The above holomorphic operators close among themselves under Operator Product Expansion (OPE) and hence generate a higher-spin type $\mathcal{W}$-algebra. A similar result holds for the anti-holomorphic operators. Moreover, for each spin we find an operator in the symmetric channel and one in the antisymmetric channel, which is identical[3] to the structure of the generators of the bosonic subalgebra of the $\mathcal{N}=2$ supersymmetric $\mathcal{SW}_{1+\infty}$ algebra that governs the symmetry of many supersymmetric higher-spin theories in 2 dimension [129, 131–135]. This spectrum is as we expected since the model has a right-moving $\mathcal{N}=2$ supersymmetry.

It is slightly more surprising that we also find conserved anti-holomorphic operators in the limit (4.1). On the other hand, the left-moving sector does not have supersymmetry; it

[3]The is one subtlety: we have one more spin-1 field in our model comparing to the generators of the $\mathcal{N}=2$ $\mathcal{SW}_{1+\infty}$ algebra. This spin-1 extended $\mathcal{N}=2$ $\mathcal{SW}_{1+\infty}$ algebra is very similar with the one withour the extra spin-1 field and is recently discussed in the context of Affine Yangian [129, 130].

JHEP12(2018)065

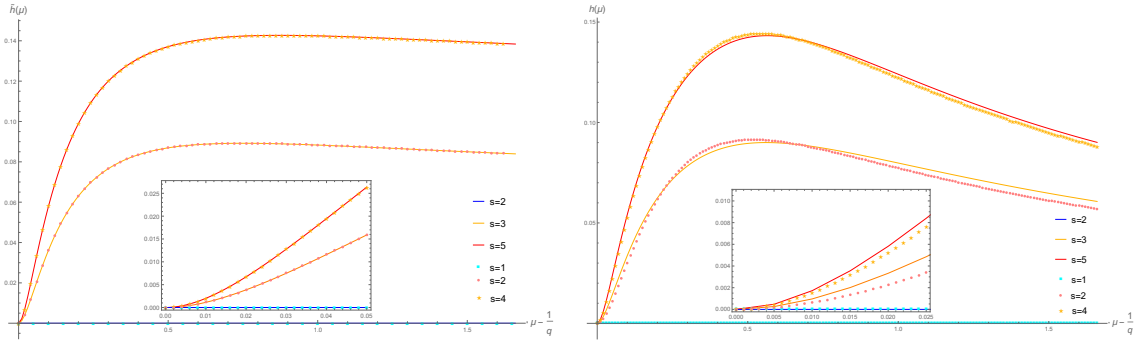

(a) Anomalous dimensions of the holomorphic higher-spin operators. Here we plot the left dimension $\tilde{h}$ of the operators and the right dimension is $h = \tilde{h} + s$.

(b) Anomalous dimensions of the anti-holomorphic higher-spin operators. Here we plot the right dimension h of the operators and the left dimension is $\tilde{h} = h + s$.

Figure 7. The dimensions of operators with integer spins as a function of μ. The smaller figure in the frame zooms in to the bottom left corner of each large figure and shows that the anomalous dimensions of these operators approach zero in the limit $\mu \to \left(\frac{1}{q}\right)^+$. The solid curves denotes operators in the symmetric channel, the discrete data points denote the operators in the antisymmetric channel. The plots are computed for $q = 3$. The $\mathcal{N} = (0, 2)$ supersymmetry is manifest in the plots.

only has bosonic higher-spin symmetry emerging, which is consistent with the $\mathcal{N} = (0, 2)$ supersymmetry of our model.

Anomalous dimensions. As we go away from the limit (4.1), namely as μ becomes larger, this emergent higher-spin symmetry is broken, which is characterized by the anomalous dimensions acquired to those (anti-)holomorphic operators. This is another way to interpret figure 7, in particular the small figures inside figure 7. Before analyzing the results, we first remind the reader that in the following we call the operators that become the (anti-)holomorphic in the higher-spin limit $\mu \to \left(\frac{1}{q}\right)^+$ "almost (anti-)holomorphic higher-spin operators", even after we move away from the higher-spin limit (4.1) at generic μ. We keep in mind that they are only strictly related to conserved currents in the limit (4.1).

Coming back to the results, in figure 7a we plot the anomalous dimension of the holomorphic higher-spin operators in the symmetric channel (solid lines) and the antisymmetric channel (discrete points). We observe that for the holomorphic higher-spin operators, the anomalous dimension of a spin-s operator in the antisymmetric channel is identical to the anomalous dimension of a spin-$(s+1)$ operator in the symmetric channel. This is consistent with the $\mathcal{N} = 2$ supersymmetry in the right-moving section: the two operators are respectively the top and the bottom component of a single multiplet that consists of operators with spin $(s, s + \frac{1}{2}, s + 1)$.[4] This confirms that the right-moving $\mathcal{N} = 2$ supersymmetry is always perserved at generic value of μ.

[4]Notice that we have implicitly used the shadow representation of the 4-point functions. So each solution to the equation (3.28) correspond to an SL(2) primary field. On the other hand, since we are not using the superspace formalism and directly work with the component fields in each supermultiplet, the eigenfunctions/operators we found could be supersymmetric descendant fields.

JHEP12(2018)065

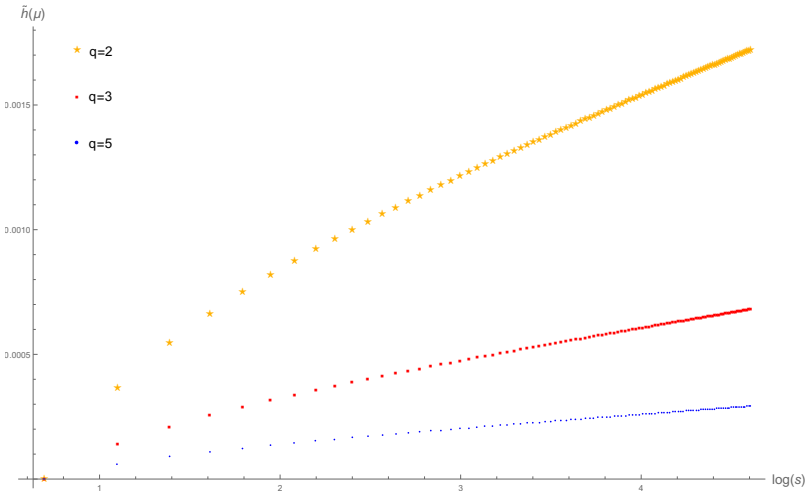

Figure 8. The anomalous dimension of the higher spin operators as a function of the spin of the operators. The yellow stars, red dots and the blue crosses are for $q = 2, 3, 5$ respectively and $\mu q - 1 = \epsilon = 0.01$. The horizontal axis is $\log(s)$ where s is the spin of the operator. The vertical axis is the anomalous dimension. It is observed that when s is relatively large, the anomalous dimension is propotional to the log of the spin. This is the same behavior as the result from a perturbative higher-spin CFT computation [136], as well as the dispersion relation of a classical rotating string in AdS spacetime in the large-spin limit [137].

On the other hand, from figure 7b we observe that there is no such relation among the almost anti-holomorphic operators in the symmetric and antisymmetric channels away from the limit (4.1). This is again compatible with the fact that there is no supersymmetry in the left-moving sector.

It is also illustrative to study the dispersion relation, namely to understand how do the anomalous dimensions, which is the same as $\tilde{h}$ for the anti-holomorphic higher-spin operators or h for the holomorphic higher-spin operators, depend on the spin once we move away from the higher spin limit. One can find this by solving

$$E_c(\pm 1, \tilde{h} + s, \tilde{h}, \frac{1+\epsilon}{q}, q) = 0\,, \qquad \epsilon \ll 1\,, s > 0\,, \tag{4.6}$$

to determine the implicit function $\tilde{h}^\epsilon(s)$. And similarly the implicit function $h^\epsilon(s)$ for the anti-holomorphic operators. This is again easily achieved numerically. The result for the anomalous dimension of the almost holomorphic higher-spin operators in the symmetric channel is plotted in figure 8. The results for the operators in the antisymmetric channel and the anti-holomorphic operators have similar structure. In figure 8 we observe that for each given q, the anomalous dimension $\gamma_\epsilon(s) = \tilde{h}_\epsilon(s)$ behaves like

$$\tilde{h}_\epsilon(s) \sim \log(s)\,, \tag{4.7}$$

for relative large spin s near the higher-spin limit (4.1). This result, which comes from diagonalizing the kernels of the SYK model and taking a higher-spin limit (4.1), agrees well with the result from a direct higher-spin CFT perturbation computation [136], as well

JHEP12(2018)065

as the dispersion relation of a classical rotating string in AdS spacetime in the large-spin regime [137]. This agreement means we have a consistent picture describing the properties of a model with an approximate higher-spin symmetry: we get the same results by either going away from a theory with exact higher-spin symmetry or going towards a higher-spin limit from a model that does not have a higher-spin symmetry. Since our computation is from a different approach, it serves as an independent evidence to support the general picture that the SYK-like models can be related to some finite tension string theory, while the higher-spin theories can be regarded as some (truncation of) tensionless string theory. In our model tuning the μ parameter away from the limit (4.1) drives the model from a higher-spin-like regime to SYK-like regime, which mimics the process of turning on the string tension.

The Lyapunov exponent. The higher-spin limit $\mu \to \left(\frac{1}{q}\right)^+$ is also detected from the chaotic behavior. Indeed the Lyapunov exponent vanishes in the limit $\mu \to \left(\frac{1}{q}\right)^+$ as can be seen from figure 6a and figure 12. This vanishing Lyapunov exponent agrees with previous expectations that theories with an infinite dimensional higher-spin symmetry is not chaotic [6, 25, 138].

The q-dependence. A further comment is about the relative magnitude of the anomalous dimensions for different q. We notice that the anomalous dimensions become smaller as q becomes larger. This is what we expected for many previously studied SYK-like models; the larger the value of q the less relevant the interaction. Consequently, we expect the anomalous dimensions to be smaller for a larger q.

This is a singular limit. A last comment is that this $\mu \to (\frac{1}{q})^+$ limit is singular: one cannot naively take all the formula and plug in $\mu = \frac{1}{q}$ since the Fourier transform (2.36) diverges. Instead one has to consider setting $\mu = \frac{1}{q} + \delta$ with $1 \gg \delta > 0$ and extract the result by taking the limit $\epsilon \to 0$, which is how all the above results are computed. It is not very surprising that the higher-spin limit is singular: we have learned from many other cases that the higher-spin limit of different models are often singular [139–141], see [142–145] for recent development. A different way to phase the singular nature of this limit is that the system undergoes a phase transition when going into/away from this limit. This is a first order phase transition because the free energy of the system, which can be expressed in terms of the IR propagators similar to [5–7], is discontinuous in this limit. We call this a "classical chiral" limit since the chiral mulitplet has classical dimension. But this is not quite a free field limit since the coupling remains large in this limit and the dimension of the Fermi multiplet does not take its classical/free value.

4.2 The $\mu \to +\infty$ ("classical Fermi") limit

We can consider a different limit

$$\mu \to +\infty\,, \tag{4.8}$$

JHEP12(2018)065

	holomorphic operators	anti-holomorphic operators
symmetric channel	$(h,\tilde{h})=(s,0),\ s\geq 2,\ q=2$	$(h,\tilde{h})=(0,s)\ ,\ s\geq 1$
antisymmetric channel	$(h,\tilde{h})=(s,0),\ s\geq 1,\ q=2$	$(h,\tilde{h})=(0,s)\ ,\ s\geq 1$

Table 2. The conserved operators in the limit (4.8).

where the IR dimension of the various fields are

$$\lim_{\mu\to+\infty} h_\phi=\frac{1}{2q}\,,\quad \lim_{\mu\to+\infty} h_\psi=\frac{1+q}{2q}\,,\quad \lim_{\mu\to+\infty} h_\lambda=0\,,\quad \lim_{\mu\to+\infty} h_G=\frac{1}{2} \tag{4.9}$$

$$\lim_{\mu\to+\infty} \tilde{h}_\phi=\frac{1}{2q}\,,\quad \lim_{\mu\to+\infty} \tilde{h}_\psi=\frac{1}{2q}\,,\quad \lim_{\mu\to+\infty} \tilde{h}_\lambda=\frac{1}{2}\,,\quad \lim_{\mu\to+\infty} \tilde{h}_G=\frac{1}{2}\,. \tag{4.10}$$

In this limit another tower of higher-spin operators emerges. To illustrate this we carry out a set of computation that is in parallel with what we have done in the previous subsection.

A tower of higher-spin operators. As in the previous limit (4.1), we look for holomorphic operators with dimension $(h,\tilde{h})=(s,0)$ and anti-holomorphic operators with dimension $(h,\tilde{h})=(0,s)$ in both the symmetric and antisymmetric channels of the limit (4.8). This amounts to solve

$$\lim_{\mu\to+\infty} E_c(\pm 1,\tilde{h}+s,\tilde{h},\mu,q)=0\,,\quad \lim_{\mu\to+\infty} E_c(\pm 1,h,h+s,\mu,q)=0\,,\quad s\in\mathbb{Z}_+\,. \tag{4.11}$$

Numerically we get a function $\tilde{h}(\mu)$ or $h(\mu)$ for any given s and q. The emergent conserved higher-spin operators are summarized in table 2. Therefore, we find a set of holomorphic higher-spin operators in the right-moving sector only at $q=2$. This spectrum matches with the spectrum of generators of the bosonic subalgebra of the $\mathcal{N}=2$ $\mathcal{SW}_{1+\infty}$ algebra. This is again consistent with the $\mathcal{N}=2$ supersymmetry in the right-moving sector. In addition, we find a tower of higher-spin operators in the left-moving sector for any $q>1$. Therefore we expect an $\mathcal{N}=(0,2)$ supersymmetric higher-spin symmetric in the limit (4.8) at $q=2$. Therefore at $q=2$ we find both the holomorphic and anti-holomorphic conserved higher spin operators at each integer spin s. But for other $q>2$, we only find anti-holomorphic higher-spin operators that generate an anti-chiral bosonic $\mathcal{W}_{1+\infty}$ algebra in the left-moving sector. Notice that this tower of chiral higher-spin operators is slightly unfamiliar since a general conserved higher-spin currents should have both the holomorphic and anti-holomorphic components. Therefore we believe the tower of higher-spin operators at $q=2$ are related to the usual higher-spin currents that generate the higher-spin symmetry.

Some examaples of the dimensions of the holomorphic higher-spin operators are shown in figure 9a, where we plot the left dimension $\tilde{h}$ of the spin-s operators both in the symmetric (solid lines) and the antisymmetric (discrete points) channels as a function of $\frac{1}{\mu}$ for the whole range of $\frac{1}{\mu}$. From this result we indeed see that in the $\mu\to+\infty$ limit the left dimension $\tilde{h}_s(\mu)$ all approach zero, which indicates that there is a tower of holomorphic operators with dimension $(h,\tilde{h})=(s,0)$. We also plot the anomalous dimension of the anti-holomorphic operators in figure 10. We do not see any coincidence of the dimensions

JHEP12(2018)065

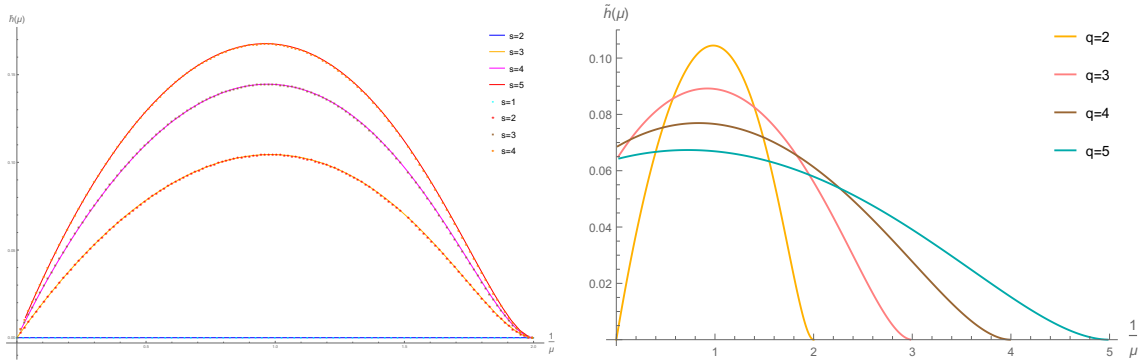

(a) The $q = 2$ case. The anomalous dimension of the higher-spin operators vanish in the limit $\mu \to \infty$. They become conserved higher-spin currents in this limit. The spin-2 operator, namely the stress-energy tensor, is always conserved for the whole range of μ where our SYK solution is reliable.

(b) The $q \neq 2$ cases. The curves are the anomalous dimension of the spin $s = 3$ operator as a function of μ. The operator has nonvanishing anomalous dimension and are not conserved as $\mu \to +\infty$. The behavior of the operators in the antisymmetric channel are similar.

Figure 9. The anomalous dimension of the almost holomorphic higher-spin operators as a function of $\frac{1}{\mu}$ for the entire range of μ.

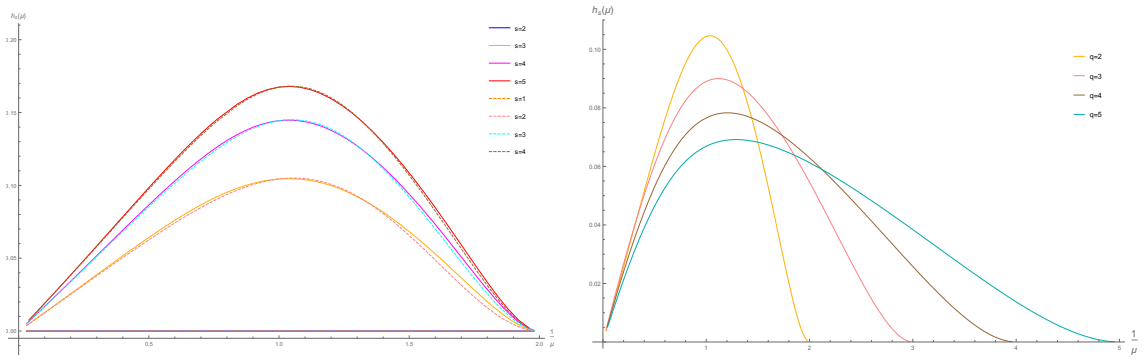

(a) The $q = 2$ case.

(b) General q.

Figure 10. Anomalous dimension of the anti-holomrphic higher-spin operators. The solid curves are for operators in the symmetric channel and the dashed lines are for operators in the antisymmetric channel. The plot is for $q = 3$. No overlapping of the solid and dashed curves are obvserved, which reflects the absence of supersymmetry in the left-moving sector.

between the symmetric and antisymmetric channels. This indicates that in the infrared the model only has $\mathcal{N} = (0, 2)$ supersymmetry, namely there is no supersymmetry in the left-moving section, away from the higher-spin limits (4.1) and (4.8).

The q-dependence. We notice that the tower of holomorphic higher-spin operators only emerges at $q = 2$. We have solved the equation

$$\lim_{\mu \to +\infty} E_c(1, \tilde{h} + s, \tilde{h}, \mu, q) = 0\,, \tag{4.12}$$

JHEP12(2018)065

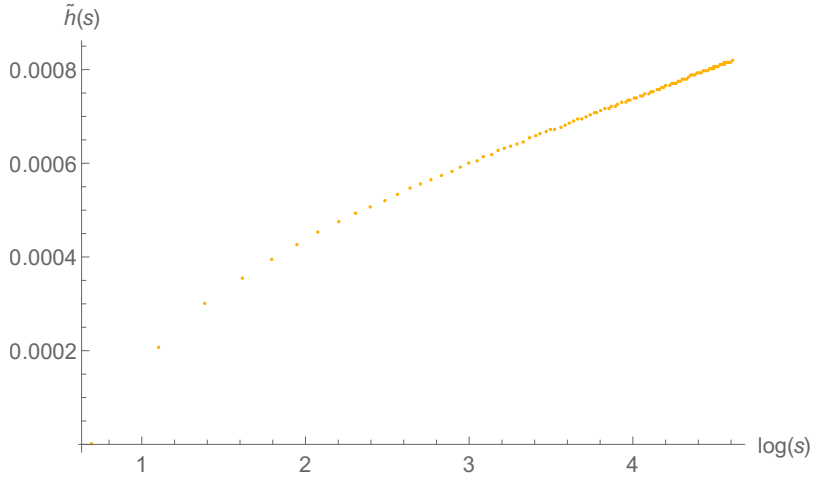

Figure 11. The anomalous dimension of the higher-spin operators as a function of their spin. The plot is around the higher-spin limit (4.8). We observe that for large enough spin the anomalous dimension is proportional to the log of the spin.

for a few different q's and we find that the operators with higher spin have nonvanishing anomalous dimension for all $q > 2$. This is shown in figure 9b. We do not have a good physical explanation of why $q = 2$ is special in this sense.[5] For completeness we list the dimensions of the chiral and Fermi multiplet in the limit (4.8) at $q = 2$

$$\lim_{\mu\to+\infty,q=2} h_\phi = \frac{1}{4}\,, \quad \lim_{\mu\to+\infty,q=2} h_\psi = \frac{3}{4}\,, \quad \lim_{\mu\to+\infty,q=2} h_\lambda = 0\,, \quad \lim_{\mu\to+\infty,q=2} h_G = \frac{1}{2} \tag{4.13}$$

$$\lim_{\mu\to+\infty,q=2} \tilde{h}_\phi = \frac{1}{4}\,, \quad \lim_{\mu\to+\infty,q=2} \tilde{h}_\psi = \frac{1}{4}\,, \quad \lim_{\mu\to+\infty,q=2} \tilde{h}_\lambda = \frac{1}{2}\,, \quad \lim_{\mu\to+\infty,q=2} \tilde{h}_G = \frac{1}{2}\,. \tag{4.14}$$

We notice that in the limit (4.8) the chiral multplet gets its largest possible dimension at $q = 2$.

Anomalous dimensions. The anomalous dimensions again have a logarithmic dependence on the spin, as can be seen from figure 11. This is similar to the behavior in the other limit (4.1) and agrees with the result from pure higher-spin theory computation [136]. We only plot the holomorphic operators in the symmetric channel; the holomorphic operators in the anti-symmetric channel are in the same supermultplets and have identical anomalous dimensions.

The Lyapunov exponent. We can compute the Lyapunov exponent of our model for the whole range of μ. We find vanishing Lyapunov exponent at $\mu \to \infty$ only for $q = 2$, which can be observed in figure 12. This is compatible with the fact that a normal higher-spin symmetry emerges in this limit only at $q = 2$, as we have discussed above.

This is a singular limit. The limit (4.8) is singular for a similar reason as the limit (4.1): the result depends on how the limit is taken. In the above analysis, we solve for the anomalous dimension at a given μ around $\mu \to +\infty$ and track how does this anomalous

[5] We remind the reads that our model (2.26) is not free at $q = 2$. Instead the interaction becomes a random mass term at $q = 1$.

JHEP12(2018)065

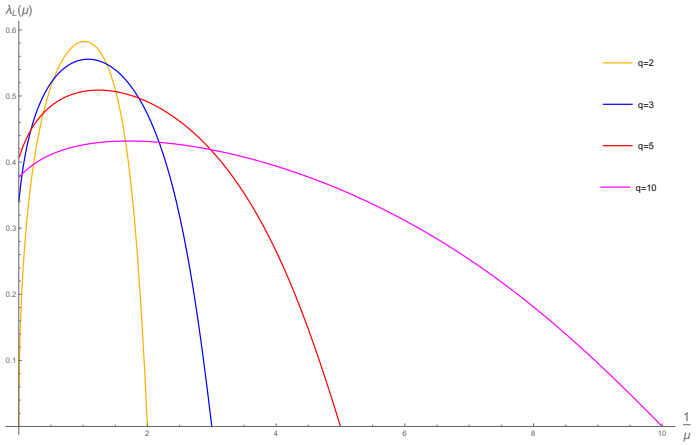

Figure 12. The Lyapunov exponent as a function of μ for the whole range of μ. We observe that near the $\mu \to +\infty$ limit only the model with $q = 2$ has a vanishing Lyapunov exponent. This is consistent with the fact that only at $q = 2$ the set of higher-spin operators have vanishing anomalous dimension and generate a higher-spin symmetry.

dimension behave as μ approaches $+\infty$. If we instead take an unphysical approach by simply plugging $\frac{1}{\mu} = 0$ and $h = 0$ (or $\tilde{h} = 0$) into the equation (3.28), we are not guaranteed to get the same result. In addition, in this computation we have first assumed the μ to be finite, solve the set of Schwinger-Dyson equations, and then take the $\mu \to \infty$ limit of the solution. We do not expect to recover the same result if we first take a naive $\mu \to +\infty$ limit of the Schwinger-Dyson equation and then solve it. As in the previous limit (4.1), we believe this subtlety reflects the common feature that a tensionless limit of string theory is usually singular and the model undergoes a first order phase transition in this limit.

4.3 Relations with higher-spin theories

Our model is defined in 2-dimensions where conformal field theories with higher-spin symmetries and their holographic dual have been extensively studied, see e.g. [146] for a review. In a supersymmetric context, the higher-spin conserved currents generate a supersymmetric $\mathcal{SW}_\infty$-algebras. It is well known that the $\mathcal{SW}_\infty$ algebra allows a continuous deformation that preserves the higher-spin symmetry; there is a family of higher-spin $\mathcal{SW}_\infty[\lambda]$ algebra. In our model there are two parameters. As we have shown in previous sections, the μ parameter controls the breaking of the higher-spin symmetry. While in the higher-spin limit (4.1), there is no requrement of the q paramter: the higher-spin symmetry emerges at any given $q > 2$. It is thus natural to conjecture that the different higher-spin algebras emerging in the models with different q should be identified with the $\mathcal{SW}_\infty[\lambda(q)]$ algebras via an explict map $\lambda = \lambda(q)$. At the moment we have not yet identified this map. We plan to study this point in detail in future works. In figure 13 we draw a cartoon summarizing the properties of the model (2.26) on the moduli space spanned by the q and μ paramerters. On the graph we mark out the two limits where higher-spin symmetries emerge. Outside the shaded region the Fourier transform in (2.36) diverges. As suggested in [101] one probably has to turn on a negative mass counterterm to reach another fixed

JHEP12(2018)065

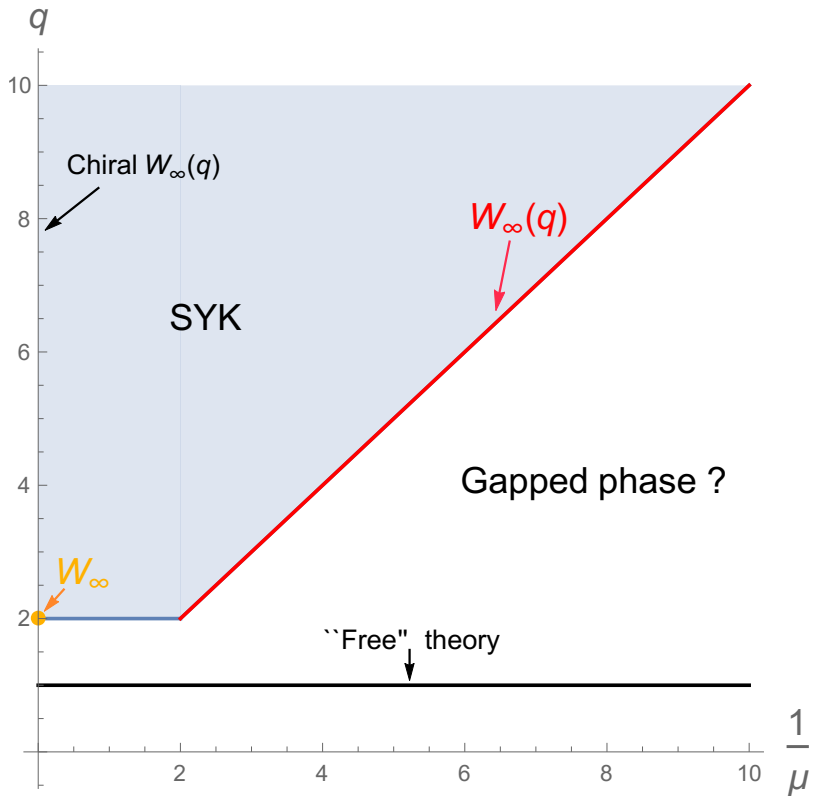

Figure 13. An illustration of the moduli space of our model. In the shaded region the model has SYK-like behavior. In the two limits, which are on the boundary of the shaded region, one observe emergent higher-spin symmetries. At $q = 1$, the interaction is quadratic, which can be regarded as a free "mass" term and the model is essentially free. Outside the shaded region the Fourier transform in (2.36) diverges. As suggested in [101] one probably has to turn on a negative mass counterterm to reach another fixed point. This is an indication that in this region the model might be gapped.

point. This is an indication that in this region the model might be gapped. It is interested to clarify this point further, and we will defer this into future works.

The existence of the μ parameter and the appearance of a higher-spin limit as we vary μ has some resemblance to the ABJ triality [147] in one dimension higher. In our model there are indeed two global symmetry $\mathrm{U}(N) \times \mathrm{U}(M)$ corresponding to the rotations of the N chiral multiplets and the M Fermi multiplets respectively. Notice that this symmetry is only manifest once we average over the random coupling. Furthermore since we consider only singlets under these two global symmetry groups, we do not expect the results discussed in this paper to alter significantly once we gauge the $\mathrm{U}(N) \times \mathrm{U}(M)$ group [96]. As a result, tuning our parameter μ to reach limits with higher-spin symmetries has a qualitative similarity with, in the context of the ABJ triality, dialing the ratio $\frac{M}{N}$ to reach a conjectured dual of $\mathcal{N} = 6$ matrix extended Vasiliev higher-spin theory [147]. But there are also qualitative differences between our model and the case of the ABJ triality. Firstly, the ABJ theory consists of (anti-)bifundamental fields, while our model (2.26) is built from (anti-)fundamental fields of the two global symmetry groups. Therefore we

JHEP12(2018)065

expect a different mechanism of the emergence of the higher-spin fields. Secondly, as the ratio $\frac{M}{N}$ increases there are two phase transitions separating three different phases with different thermodynamic properties [147]. But in our model, at least for $q = 2$, as we increase μ the model moves from a higher-spin behavior to a chaotic SYK-like behavior and then back to a higher-spin behavior (although a different one comparing to where the model started).

There could be other parameters that we can turn on while maintaining the properties of the models we have discussed in this paper. Notice that this possibility goes along with our previous analysis based on the chaotic behavior of this model, where the fact that the Lyapunov exponent does not saturate the chaos bound [26] could be a hint that there should be other directions on the moduli space of 2d SYK-like models along which the model ets more and more chaotic.

Acknowledgments

We thank Ksenia Bulycheva, Anthony Charles, Wenbo Fu, Ping Gao, Harsha Hampapura, Thomas Hartman, Antal Jevicki, Shota Komatsu, Eric Marcus, Daniel Mayerson, Leopoldo Pando Zayas, Eric Perlmutter, Vimal Rathee, Marcus Spradlin, Stefan Stanojevic, Bogdan Stoica, Grigory Tarnopolsky, Anastasia Volovich, Cenke Xu, Zhenbin Yang, Wenli Zhao and Alexander Zhiboedov for discussions on related topics. We are especially grateful to Juan Maldacena and Douglas Stanford for illuminating discussions. In particular we thank Douglas Stanford for sharing a code based on which the numerical analysis in section 2.2 is developed. We thanks the Leinweber Center for Theoretical Physics of University of Michigan, Ann Arbor and the Institute for Advanced Study for hospitality at different stages of this project. This work was supported by the US Department of Energy under contract DE-SC0010010 Task A.

A 2d SYK model with $\mathcal{N} = (2, 2)$ supersymmetry

In 2 dimension, the $\mathcal{N} = (2, 2)$ superfields are constructed with the help of two complex fermionic coordinates θ^+ and θ^- with

$$\bar{\theta}^{\pm} = (\theta^{\pm})^* \,. \tag{A.1}$$

A bosonic chiral superfield is defined as

$$\Phi(x^i, \theta^{\pm}, \bar{\theta}^{\pm}) = \phi(y^{\pm}) + \sqrt{2}\theta^+\psi(y^{\pm}) + \sqrt{2}\theta^-\lambda(y^{\pm}) + 2\theta^+\theta^- F(y^{\pm}) \,, \tag{A.2}$$

where $y^{\pm} = x^{\pm} - i\theta^{\pm}\bar{\theta}^{\pm}$. A simple 2d SYK-like model with $\mathcal{N} = (2, 2)$ supersymmetry is [101, 112]

$$S = \int dx^2 d^2\theta^+ d^2\theta^- \Phi\bar{\Phi} + \int dx^2 d\theta^+ d\theta^- \left(\frac{J_{i_0 \ldots i_q}}{(q+1)!} \Phi^{i_0} \ldots \Phi^{i_q} + \text{h.c.} \right) \tag{A.3}$$

JHEP12(2018)065

In component form the interaction is

$$S_{\rm int}^{(0,0)} = \int dx^2 \left(\frac{J_{i_0 \ldots i_q}}{q!} F^{i_0} \phi^{i_1} \ldots \phi^{i_q} + \frac{J_{i_0 \ldots i_q}}{q!} \psi^{i_0} \lambda^{i_1} \phi^{i_3} \ldots \phi^{i_q} + \text{h.c.} \right) . \tag{A.4}$$

It is straightforward to solve the Schwinger-Dyson equation of the two point functions in the IR limit

$$\int d^2 z_2 G_c^I(z_1, z_2) \Sigma_c^I(z_2, z_3) = -\delta^2(z_1 - z_3) , \qquad I = \phi , \psi , \lambda , G , \tag{A.5}$$

where $G_c^I(z_1, z_2)$ are the propagators in the infrared and $\Sigma_c^I(z_1, z_2)$ are the corresponding self-energies of the various fields

$$\Sigma^{\psi}(z_1, z_2) = 2J^2 G^{\lambda}(z_1, z_2)(G^{\phi}(z_1, z_2))^{q-1} \tag{A.6}$$

$$\begin{aligned} \Sigma^{\phi}(z_1, z_2) = {} & (q-1) 2J^2 (G^{\phi}(z_1, z_2))^{q-2} G^{\lambda}(z_1, z_2) G^{\psi}(z_1, z_2) \\ & + 2J^2 (G^{\phi}(z_1, z_2))^{q-1} G^{G}(z_1, z_2) , \end{aligned} \tag{A.7}$$

$$\Sigma^{G}(z_1, z_2) = \frac{2J^2}{q} (G_c^{\phi}(z_1, z_2))^q , \tag{A.8}$$

$$\Sigma^{\lambda}(z_1, z_2) = 2J^2 (G_c^{\phi}(z_1, z_2))^{q-1} G_c^{\psi}(z_1, z_2) . \tag{A.9}$$

A supersymmetric solution of these equations reads

$$G_c^{\phi}(z_1, z_2) = \left(\frac{q}{8\pi^2 J^2} \right)^{\frac{1}{q+1}} (z_1 - z_2)^{-\frac{1}{q+1}} (\bar{z}_1 - \bar{z}_2)^{-\frac{1}{q+1}} , \tag{A.10}$$

and the other propagators are related by supersymmetry

$$G^{\psi}(z_1, z_2) = -2\partial_{z_1} G^{\phi}(z_1, z_2) , \qquad G^{\lambda}(z_1, z_2) = -2\partial_{\bar{z}_1} G^{\phi}(z_1, z_2) \tag{A.11}$$

$$G^{G}(z_1, z_2) = -2\partial_{z_1} G^{\lambda}(z_1, z_2) = -2\partial_{\bar{z}_1} G^{\psi}(z_1, z_2) . \tag{A.12}$$

The existence of such solutions is nontrivial. Indeed one can write down a similar set of Schwinger-Dyson equations for various models without supersymmetry [101], but it is not clear if the theory actually flows to the assumed SYK-like IR fixed points. The presence of supersymmetry improves the UV behavior and the potential divergences are avoided. In practice, the supersymmetry allows a natural regularization and renormalization of the possible divergences in a naive direct solution.

For later purpose it is useful to recast the $\mathcal{N} = (2, 2)$ model (A.3) as a model with a smaller number of supersymmetry. In terms of the $\mathcal{N} = (0, 2)$ superfields

$$\text{chiral:} \quad \Phi'^i(x, \theta^+) = \Phi^i(y, \theta^{\pm}, \bar{\theta}^{\pm})\big|_{\theta^-, \bar{\theta}^- \to 0} = \phi(x) + \sqrt{2}\theta^+ \psi(x) + 2\theta^+ \bar{\theta}^+ \partial_z \phi(x) \tag{A.13}$$

$$\text{Fermi:} \quad \Lambda(x, \theta^+)^i = D_- \Phi^i(y, \theta^{\pm})\big|_{\theta^- \to 0} = \lambda(x) - \sqrt{2}\theta^+ F(x) + 2\theta^+ \bar{\theta}^+ \partial_z \psi_-(x) , \tag{A.14}$$

where $D_- = \frac{\partial}{\partial \theta^-} + 2\bar{\theta}^- \partial_z$ and the action can be written as

$$S^{(0,2)} = \int dx^2 d\theta^+ d\bar{\theta}^+ \left(\frac{1}{2} \bar{\Lambda} \Lambda - \bar{\Phi} \partial_{\bar{z}} \Phi \right) + \int d\theta^+ \frac{J_{i_0 \ldots i_q}}{q!} \Lambda^{i_0} \Phi^{i_1} \ldots \Phi^{i_q} + \text{h.c.} . \tag{A.15}$$

JHEP12(2018)065

B Perturbing the $\mathcal{N}=(2,2)$ model to the $\mathcal{N}=(0,2)$ models

In this section, we treat the $\mathcal{N}=(0,2)$ model as a perturbation of the $\mathcal{N}=(2,2)$ model. We then solve the $\mathcal{N}=(0,2)$ model perturbatively around the $\mathcal{N}=(2,2)$ fixed point. We will show that the result from this perturbative analysis does agree with the $\mu \to 1$ expansion of the result in section 2.2. Since the computation in this section is independent from directly solving the Schwinger-Dyson equations in section 2.2, the results in this section provide another consistency check of the results in the main text.

The perturbed theory has the same action as in section 2.2, the only difference is that now we take the ratio $\mu = M/N$ to be $\mu = 1+\epsilon$, where $\epsilon \ll 1$ is treated as a small parameter, and we expand the propagators of the deformed model as

$$G^I(x) = G^I_c(x)(1+\epsilon g^I(x)+\ldots)\,, \qquad I=\phi,\psi,\lambda,G\,. \tag{B.1}$$

In frequency domain, the perturbation can be denoted as

$$G^I(p) = G^I_c(p) + \epsilon\left(\widetilde{G^I_c \times g^I}\right)+\ldots\,, \tag{B.2}$$

where $\widetilde{\ }$ indicates a Fourier transform. The self energies of the deformed model are, to the leading order in ϵ

$$\begin{aligned}
\Sigma^\psi(z_1,z_2) &= 2J^2(1+\epsilon)G^\lambda(z_1,z_2)(1+\epsilon g^\lambda(z_1,z_2))(G^\phi(z_1,z_2))^{q-1}(1+\epsilon g^\phi(z_1,z_2))^{q-1} && \text{(B.3)}\\
&= \Sigma^\psi(z_1,z_2)_c\left(1+\epsilon(1+g^\lambda+(q-1)g^\phi)\right)\,, && \text{(B.4)}\\
\Sigma^\phi(z_1,z_2) &= (q-1)2(1+\epsilon)J^2(G^\phi(z_1,z_2))^{q-2}G^\lambda(z_1,z_2)G^\psi(z_1,z_2)\\
&\quad +2J^2(1+\epsilon)(G^\phi(z_1,z_2))^{q-1}G^G(z_1,z_2)\,, && \text{(B.5)}\\
&= \frac{q-1}{q}\Sigma^\phi_c\left(1+\epsilon(1+g^\lambda+g^\psi+(q-2)g^\phi)\right)+\frac{1}{q}\Sigma^\phi_c\left(1+\epsilon(1+g^G+(q-1)g^\phi)\right) && \text{(B.6)}\\
\Sigma^G(z_1,z_2) &= \frac{2J^2}{q}(G^\phi_c(z_1,z_2))^q\left(1+\epsilon q g^\phi\right) = \Sigma^G_c(z_1,z_2)\left(1+\epsilon q g^\phi\right)\,, && \text{(B.7)}\\
\Sigma^\lambda(z_1,z_2) &= 2J^2(G^\phi_c(z_1,z_2))^{q-1}G^\psi_c(z_1,z_2)\left(1+\epsilon(g^\psi+(q-1)g^\phi)\right) && \text{(B.8)}\\
&= \Sigma^\lambda(z_1,z_2)\left(1+\epsilon(g^\psi+(q-1)g^\phi)\right)\,. && \text{(B.9)}
\end{aligned}$$

Because we are perturbing around the SYK fix point in the IR, we solve the Schwinger-Dyson equations of the perturbed model

$$G^I(p)\Sigma^I(p) = -1\,, \tag{B.10}$$

with the known results of the unperturbed ones

$$G^I_c(p)\Sigma^I_c(p) = -1\,. \tag{B.11}$$

This leads to

$$G^I_c(p)\delta\Sigma^I(p) + \delta G^I(p)\Sigma^I_c(p) = 0\,, \tag{B.12}$$

JHEP12(2018)065

where $\delta G^I(p) = G^I(p) - G^I_c(p)$ and $\delta\Sigma^I(p) = \Sigma^I(p) - \Sigma^I_c(p)$. In components, the equations are

$$-1 = G^\psi_c(p)\left(\widetilde{\Sigma^\psi_c \times g^\lambda} + (q-1)\widetilde{\Sigma^\psi_c \times g^\phi}\right) + \Sigma^\psi_c(p)\widetilde{G^\psi_c \times g^\psi} \tag{B.13}$$

$$-1 = G^\phi_c(p)\left(\frac{q-1}{q}\widetilde{\Sigma^\phi_c \times g^\lambda} + \frac{q-1}{q}\widetilde{\Sigma^\phi_c \times g^\psi} + \frac{1}{q}\widetilde{\Sigma^\phi_c \times g^G}\right. \tag{B.14}$$

$$\left. + \frac{q^2-2q+1}{q}\widetilde{\Sigma^\phi_c \times g^\phi}\right) + \Sigma^\phi_c(p)\widetilde{G^\phi_c \times g^\phi} \tag{B.15}$$

$$0 = G^\lambda_c(p)\left(\widetilde{\Sigma^\lambda_c \times g^\psi} + (q-1)\widetilde{\Sigma^\lambda_c \times g^\phi}\right) + \Sigma^\lambda_c(p)\widetilde{G^\lambda_c \times g^\lambda} \tag{B.16}$$

$$0 = G^G_c(p)\left(q\widetilde{\Sigma^G_c \times g^\phi}\right) + \Sigma^G_c(p)\widetilde{G^G_c \times g^G}\,. \tag{B.17}$$

Now we look for a solution of the above equations with $\mathcal{N} = (0,2)$ supersymmetry, which means

$$\widetilde{G^G_c \times g^G} = i\bar{p}\widetilde{G^\lambda_c \times g^\lambda}\,, \qquad \widetilde{G^\psi_c \times g^\psi} = i\bar{p}\widetilde{G^\phi_c \times g^\phi}\,. \tag{B.18}$$

These relations simplify (B.16) to

$$\left(\widetilde{\Sigma^\lambda_c \times g^\psi} + (q-1)\widetilde{\Sigma^\lambda_c \times g^\phi}\right) = i\bar{p}\left(q\widetilde{\Sigma^G_c \times g^\phi}\right)\,. \tag{B.19}$$

Now we can Fourier transform back to get

$$\Sigma^\lambda_c \times g^\psi + (q-1)\Sigma^\lambda_c \times g^\phi = -2q\partial_z\left(\Sigma^G_c \times g^\phi\right) = -2q\partial_z\Sigma^G_c \times g^\phi - 2q\Sigma^G_c\partial_z g^\phi\,. \tag{B.20}$$

Further using

$$\Sigma^\lambda_c = -2\partial_z\Sigma^G_c\,, \qquad \Sigma^\phi_c = -2\partial_{\bar{z}}\Sigma^\psi_c\,, \tag{B.21}$$

we get

$$\Sigma^\lambda_c \times g^\psi - \Sigma^\lambda_c \times g^\phi = -2q\Sigma^G_c\partial_z g^\phi\,. \tag{B.22}$$

Multiplying by $(\Sigma^\lambda_c)^{-1}G^\psi_c$ and using the known results for the $\mathcal{N} = (2,2)$ conformal propagators and the self energies, we get

$$G^\psi_c \times g^\psi - G^\psi_c \times g^\phi = -2b^\phi(z\bar{z})^{-\frac{1}{q+1}}\partial_z g^\phi\,. \tag{B.23}$$

Then using

$$G^\psi_c \times g^\psi = -2\partial_z(G^\phi_c \times g^\phi)\,, \tag{B.24}$$

the above equation becomes

$$-2\partial_z(G^\phi_c \times g^\phi) - G^\psi_c \times g^\phi = -2b^\phi(z\bar{z})^{-\frac{1}{q+1}}\partial_z g^\phi\,. \tag{B.25}$$

Plugging in the known results for the $\mathcal{N} = (2,2)$ conformal propagators, we get a trivial identity.

JHEP12(2018)065

Similarly, the equations (B.15) turns out to be a trivial identity as well. This means that the $\mathcal{N}=(0,2)$ SUSY is compatible with the 4 equations and it further reduces those to two equations. To solve the rest 2 equations we consider the following ansatz

$$g^\phi = n^\phi + \delta^\phi \log(z\bar{z})\,, \qquad g^\lambda = n^\lambda + \delta^\lambda \log(z\bar{z})\,. \tag{B.26}$$

In the later computation, the following Fourier transform

$$\begin{aligned}\int_{-\infty}^{\infty} d^2z \frac{\log(z\bar{z})}{z^a\bar{z}^a} e^{ip\cdot z} &= \int_0^\infty dr \frac{2\log(r)}{r^{2a-1}} \int_0^{2\pi} d\theta\, e^{ipr\cos(\theta)} \\ &= 4\pi \int_0^\infty dr \frac{\log(r)}{r^{2a-1}} J_0(pr) \\ &= \frac{\pi 4^{1-a} p^{2a-2}\Gamma(1-a)(\psi^{(0)}(1-a)+\psi^{(0)}(a)-2\log(p/2))}{\Gamma(a)}\,.\end{aligned} \tag{B.27}$$

Strictly speaking, the integral on the l.h.s. is only convergent when $\frac{1}{4} < a < 1$. However, we do not worry to much about the $\frac{1}{4}$ end since it is an IR divergence and can be regulated by not going very deep in the IR. We only makes sure that $a < 1$ is satisfied in the following computation.

Using (B.27) we immediately compute

$$\widetilde{G_c^\phi \times g^\phi} = a^\phi G_c^\phi(p) + d^\phi \frac{\pi 4^{\frac{q}{q+1}}\Gamma(\frac{q}{q+1})(\psi^{(0)}(\frac{q}{q+1})+\psi^{(0)}(\frac{1}{q+1})-2\log(p/2))}{k^{\frac{2}{q+1}} p^{\frac{2q}{q+1}}\Gamma(\frac{1}{q+1})} \tag{B.28}$$

$$\widetilde{G_c^\phi \times g^\lambda} = a^\lambda G_c^\phi(p) + d^\lambda \frac{\pi 4^{\frac{q}{q+1}}\Gamma(\frac{q}{q+1})(\psi^{(0)}(\frac{q}{q+1})+\psi^{(0)}(\frac{1}{q+1})-2\log(p/2))}{k^{\frac{2}{q+1}} p^{\frac{2q}{q+1}}\Gamma(\frac{1}{q+1})}\,. \tag{B.29}$$

Similarly, we have

$$\widetilde{\Sigma_c^G \times g^\phi} = a^\phi \Sigma_c^G(p) + d^\phi \frac{k^{\frac{2}{q+1}}\Gamma(\frac{1}{q+1})(\psi^{(0)}(\frac{1}{q+1})+\psi^{(0)}(\frac{q}{q+1})-2\log(p/2))}{\pi 4^{\frac{q}{q+1}} p^{\frac{2}{q+1}}\Gamma(\frac{q}{q+1})} \tag{B.30}$$

$$\widetilde{\Sigma_c^G \times g^\lambda} = a^\lambda \Sigma_c^G(p) + d^\lambda \frac{k^{\frac{2}{q+1}}\Gamma(\frac{1}{q+1})(\psi^{(0)}(\frac{1}{q+1})+\psi^{(0)}(\frac{q}{q+1})-2\log(p/2))}{\pi 4^{\frac{q}{q+1}} p^{\frac{2}{q+1}}\Gamma(\frac{q}{q+1})} \tag{B.31}$$

In addition, we get

$$\widetilde{\Sigma_c^\psi \times g^\phi} = \frac{1+q}{q} d^\phi \Sigma_c^\psi(p) + ip\int_{-\infty}^\infty d^2z(\Sigma_c^G g^\phi e^{ip\cdot z}) = d^\phi \Sigma_c^\psi(p)\frac{1+q}{q} + ip\widetilde{\Sigma_c^G \times g^\phi} \tag{B.32}$$

$$\widetilde{\Sigma_c^\psi \times g^\lambda} = \frac{1+q}{q} d^\phi \Sigma_c^\psi(p) + ip\int_{-\infty}^\infty d^2z(\Sigma_c^G g^\phi e^{ip\cdot z}) = d^\lambda \Sigma_c^\psi(p)\frac{1+q}{q} + ip\widetilde{\Sigma_c^G \times g^\lambda} \tag{B.33}$$

$$\widetilde{G_c^\lambda \times g^\lambda} = (1+q) d^\lambda G_c^\lambda(p) + ip\int_{-\infty}^\infty d^2z(G_c^\phi e^{ip\cdot z} g^\lambda) = (1+q) d^\lambda G_c^\lambda(p) + ip\widetilde{G_c^\phi \times g^\lambda} \tag{B.34}$$

where we have used

$$G_c^\lambda = -2\partial_{\bar{z}} G_c^\phi\,, \qquad \Sigma_c^\psi = -2\partial_{\bar{z}}\Sigma_c^G\,. \tag{B.35}$$

JHEP12(2018)065

With these Fourier transformed quantities it is straightforward to solve (B.13), (B.17) and the solution is

$$\delta^{\phi} = -\frac{q}{(q-1)(q+1)^2}\,, \qquad n^{\lambda} = -\frac{q^2}{q^2-1} - qn^{\phi}\,, \qquad \delta^{\lambda} = \frac{q^2}{(q-1)(q+1)^2}\,. \tag{B.36}$$

Notice that the form of the correction is compatible with the infinitesimal form of the correction to the conformal 2-point function

$$G_{\epsilon}(z_1,z_2) = \frac{b(1+\epsilon n)}{(z_1-z_2)^{2h-\epsilon\delta}(\bar{z}_1-\bar{z}_2)^{2\tilde{h}-\epsilon\bar{\delta}}} \tag{B.37}$$

$$= \frac{b}{(z_1-z_2)^{2h}(\bar{z}_1-\bar{z}_2)^{2\tilde{h}}}(1+\epsilon(n+\delta\log(|z_1-z_2|^2))+\mathcal{O}(\epsilon^2))\,, \tag{B.38}$$

where we have taken $\bar{\delta}^I = \delta^I$ to retain locality. Therefore, we can rewrite the above perturbative result into an equivalent form

$$G^{\phi}_{\epsilon}(z_1,z_2) = \frac{b^{\phi}(1+\epsilon n^{\phi})}{(z_1-z_2)^{2h^{\phi}-\epsilon\delta^{\phi}}(\bar{z}_1-\bar{z}_2)^{2\tilde{h}^{\phi}-\epsilon\delta^{\phi}}}\,, \quad G^{\psi}_{\epsilon}(z_1,z_2) = -2\partial_{z_1}G^{\phi}_{\epsilon}(z_1,z_2) \tag{B.39}$$

$$G^{\lambda}_{\epsilon}(z_1,z_2) = \frac{b^{\lambda}(1+\epsilon n^{\lambda})}{(z_1-z_2)^{2h^{\lambda}-\epsilon\delta^{\lambda}}(\bar{z}_1-\bar{z}_2)^{2\tilde{h}^{\lambda}-\epsilon\delta^{\lambda}}}\,, \quad G^{G}_{\epsilon}(z_1,z_2) = -2\partial_{z_1}G^{\lambda}_{\epsilon}(z_1,z_2)\,. \tag{B.40}$$

This is compatible with the solution (2.32), (2.33) when expanded around $\mu = 1$.

C Fermionic operators in the model

In this appendix we compute some other 4-point functions in which fermionic operators propagate. From this computation we get the fermionic spectrum of the model (2.26) and observe the emergence of fermionic higher-spin operators in the two limits (4.1) and (4.8).

C.1 The $\bar{\phi}\psi$ and $\phi\bar{\psi}$ sector

We first consider the $\langle\phi^i\bar{\psi}^i\psi^j\bar{\phi}^j\rangle$ and $\langle\phi^i\bar{\psi}^iG^j\bar{\lambda}^j\rangle$ correlators. There are 6 contributing kernels

$$K^{\bar{\phi}\psi\phi\bar{\psi}}(z_1,z_2,z_3,z_4) = -2(q-1)J^2\frac{M}{N}G^{\phi}(z_{13})G^{\psi}(z_{24})(G^{\phi}(z_{34}))^{q-2}G^{\lambda}(z_{34}) \tag{C.1}$$

$$K^{\psi\bar{\phi}\bar{\psi}\phi}(z_1,z_2,z_3,z_4) = 2(q-1)J^2\frac{M}{N}G^{\psi}(z_{13})G^{\phi}(z_{24})(G^{\phi}(z_{34}))^{q-2}G^{\lambda}(z_{34}) \tag{C.2}$$

$$K^{\bar{\phi}\psi\lambda\bar{G}}(z_1,z_2,z_3,z_4) = 2J^2\frac{M}{N}G^{\phi}(z_{13})G^{\psi}(z_{24})(G^{\phi}(z_{34}))^{q-1} \tag{C.3}$$

$$K^{\psi\bar{\phi}\bar{G}\lambda}(z_1,z_2,z_3,z_4) = 2J^2\frac{M}{N}G^{\psi}(z_{13})G^{\phi}(z_{24})(G^{\phi}(z_{34}))^{q-1} \tag{C.4}$$

$$K^{\bar{\lambda}G\phi\bar{\psi}}(z_1,z_2,z_3,z_4) = 2J^2G^{\lambda}(z_{13})G^{G}(z_{24})(G^{\phi}(z_{34}))^{q-1} \tag{C.5}$$

$$K^{G\bar{\lambda}\bar{\psi}\phi}(z_1,z_2,z_3,z_4) = 2J^2G^{G}(z_{13})G^{\lambda}(z_{24})(G^{\phi}(z_{34}))^{q-1}\,. \tag{C.6}$$

The functions that diagonalize the above kernels are of the form

$$\Phi^{ij}(z_1,z_2) = (z_{12})^{h-h_i-h_j}(\bar{z}_{12})^{\bar{h}-\bar{h}_i-\bar{h}_j}\,, \tag{C.7}$$

JHEP12(2018)065

which satisfy

$$K^{ijkl} * \Phi^{\bar{i}\bar{j}} = k^{ijkl}\Phi^{ij} \,. \tag{C.8}$$

One can explicitly evaluate the integral and get

$$k^{\bar{\phi}\psi\phi\bar{\psi}} = \frac{\mu(q-1)^2 q(\mu q-1)\Gamma\left(1-2h_\phi\right)^2\Gamma\left(\frac{1}{2}-h+2h_\phi\right)\Gamma\left(\tilde{h}-1+2h_\phi\right)}{\left(\mu q^2-1\right)^2\Gamma\left(2h_\phi\right)\Gamma\left(1+2h_\phi\right)\Gamma\left(\frac{3}{2}-h-2h_\phi\right)\Gamma\left(\tilde{h}+1-2h_\phi\right)} \tag{C.9}$$

$$k^{\bar{\phi}\psi\lambda\bar{G}} = -\frac{4\pi^2 J^2\mu n_\phi^{q+1}(\mu q-1)\Gamma\left(1-2h_\phi\right)^2\Gamma\left(\frac{1}{2}-h+2h_\phi\right)\Gamma\left(\tilde{h}-1+2h_\phi\right)}{\left(\mu q^2-1\right)\Gamma\left(2h_\phi\right)\Gamma\left(1+2h_\phi\right)\Gamma\left(\frac{3}{2}-h-2h_\phi\right)\Gamma\left(\tilde{h}+1-2h_\phi\right)} \tag{C.10}$$

$$k^{\bar{\lambda}G\phi\bar{\psi}} = \frac{(q-1)^3 q^2 n_\phi^{-q-1}\Gamma\left(-2h_\lambda\right)^2\Gamma\left(\frac{1}{2}-h+2h_\lambda\right)\Gamma\left(2h_\lambda+\tilde{h}\right)}{4\pi^2 J^2\left(\mu q^2-1\right)^3\Gamma\left(2h_\lambda\right)\Gamma\left(1+2h_\lambda\right)\Gamma\left(\frac{3}{2}-h-2h_\lambda\right)\Gamma\left(\tilde{h}-2h_\lambda\right)} \tag{C.11}$$

$$k^{\psi\bar{\phi}\bar{\psi}\phi} = \frac{\mu(q-1)^2 q(\mu q-1)\Gamma\left(1-2h_\phi\right)^2\Gamma\left(\frac{1}{2}-h+2h_\phi\right)\Gamma\left(\tilde{h}-1+2h_\phi\right)}{\left(\mu q^2-1\right)^2\Gamma\left(2h_\phi\right)\Gamma\left(1+2h_\phi\right)\Gamma\left(\frac{3}{2}-h-2h_\phi\right)\Gamma\left(\tilde{h}+1-2h_\phi\right)} \tag{C.12}$$

$$k^{\psi\bar{\phi}\bar{G}\lambda} = \frac{4\pi^2 J^2\mu n_\phi^{q+1}(\mu q-1)\Gamma\left(1-2h_\phi\right)^2\Gamma\left(\frac{1}{2}-h+2h_\phi\right)\Gamma\left(\tilde{h}-1+2h_\phi\right)}{\left(\mu q^2-1\right)\Gamma\left(2h_\phi\right)\Gamma\left(1+2h_\phi\right)\Gamma\left(\frac{3}{2}-h-2h_\phi\right)\Gamma\left(\tilde{h}+1-2h_\phi\right)} \tag{C.13}$$

$$k^{G\bar{\lambda}\bar{\psi}\phi} = -\frac{(q-1)^3 q^2 n_\phi^{-q-1}\Gamma\left(-2h_\lambda\right)^2\Gamma\left(\frac{1}{2}-h+2h_\lambda\right)\Gamma\left(2h_\lambda+\tilde{h}\right)}{4\pi^2 J^2\left(\mu q^2-1\right)^3\Gamma\left(2h_\lambda\right)\Gamma\left(1+2h_\lambda\right)\Gamma\left(\frac{3}{2}-h-2h_\lambda\right)\Gamma\left(\tilde{h}-2h_\lambda\right)} \tag{C.14}$$

The final eigenvalues are obtained from diagonalizing the following matrix

$$\begin{pmatrix} 0 & 0 & k^{\bar{\phi}\psi\phi\bar{\psi}} & k^{\bar{\phi}\psi\lambda\bar{G}} \\ 0 & 0 & k^{\bar{\lambda}G\phi\bar{\psi}} & 0 \\ k^{\psi\bar{\phi}\bar{\psi}\phi} & k^{\psi\bar{\phi}\bar{G}\lambda} & 0 & 0 \\ k^{G\bar{\lambda}\bar{\psi}\phi} & 0 & 0 & 0 \end{pmatrix} \tag{C.15}$$

The expressions of the eigenvalues are not very eluminating. Here we only give the dimensions of the higher-spin operators that is of most interest to us. This is obtained in a similar manner as what we did to find the behaviors of the bosonic higher-spin operators. Namely we find the lowest dimensions, as a function of μ, that set some eigenvalue to 1 at a given spin, then we check the behavior of the dimensions as μ approaches the two limits (4.1) and (4.8). Instead of give the explicit expression of the dimensions of the operators, we simply present the results in figure 14. From the plot, we indeed observe that there is a tower of half-interger spin operators become conserved fermionic higher-spin operators in the limit (4.1) at any q. One the other hand, we only observe the emergence of the tower of conserved operators in the limit (4.8) at $q = 2$. These behavior are identical to those observed in the bosonic operators, as we expected due to supersymmetry. In adddition, the right-moving supercharges is present at any value of μ, in accord with the fact that the

JHEP12(2018)065

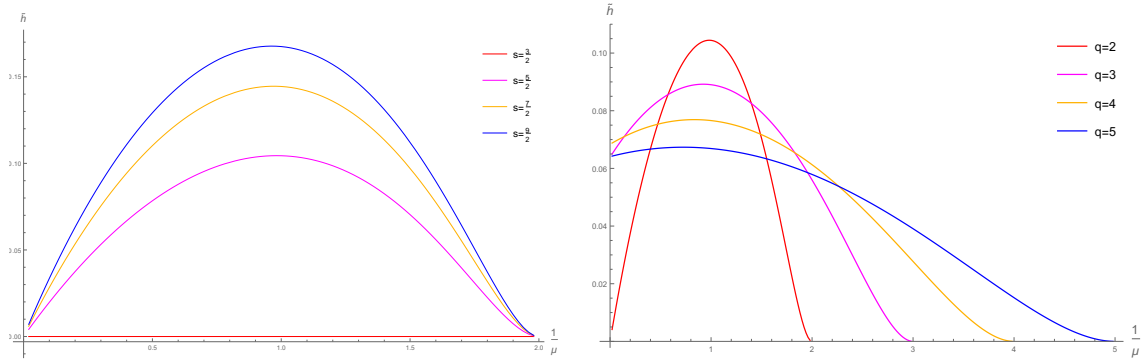

(a) The $\bar{\phi}\psi$ channel at $q = 2$. We plot the anomalous dimensions of the higher-spin operators with half-integer spin.

(b) The $\bar{\phi}\psi$ channel at general q. The curves represent the dimensions of the spin-3 operators in models with different q.

Figure 14. The lowest dimensions of the fermionic operators in the $\langle \phi^i \bar{\psi}^i \psi^j \bar{\phi}^j \rangle$ and $\langle \phi^i \bar{\psi}^i G^j \bar{\lambda}^j \rangle$ four point function. The plots illustrate how does the dimension change as a function of μ.

model has $\mathcal{N} = (0, 2)$ supersymmetry at any μ. We call the tower of higher-spin operator running in these 4-point function in the $\bar{\phi}\psi$ sector since they are expect to have the form

$$\mathcal{O}^{s+\frac{1}{2}}_{\bar{\phi}\psi} \sim \bar{\phi}^i \partial^s \psi^i + \ldots + \bar{\lambda} \partial^{s+1} G + \ldots , \tag{C.16}$$

where "..." represents other terms with different distributions of the derivatives on the two fields; the correct combination is determined by requiring the operator to be a primary field.

There is a set of conjugate kernels that gives identical eigenvalues. Hence there is a second tower of fermionic higher-spin operators appearing in the two limits (4.1) and (4.8) with identical behaviors as the parameters change. They are referred as in the $\phi\bar{\psi}$ sector. They complete the right-moving $\mathcal{N} = 2$ multiplets at each spin.

C.2 The $\bar{\phi}\lambda$ and $\phi\bar{\lambda}$ sector

We can also consider the $\langle \phi^i \bar{\lambda}^i \lambda^j \bar{\phi}^j \rangle$ and $\langle \phi^i \bar{\lambda}^i G^j \bar{\psi}^j \rangle$ correlators. There are 6 contributing kernels

$$K^{\bar{\phi}\lambda\phi\bar{\lambda}}(z_1, z_2, z_3, z_4) = -2(q-1)J^2 G^{\phi}(z_{13}) G^{\lambda}(z_{24}) (G^{\phi}(z_{34}))^{q-2} G^{\psi}(z_{34}) \tag{C.17}$$

$$K^{\lambda\bar{\phi}\bar{\lambda}\phi}(z_1, z_2, z_3, z_4) = 2(q-1)J^2 G^{\lambda}(z_{13}) G^{\phi}(z_{24}) (G^{\phi}(z_{34}))^{q-2} G^{\psi}(z_{34}) \tag{C.18}$$

$$K^{\bar{\phi}\lambda\psi\bar{G}}(z_1, z_2, z_3, z_4) = 2J^2 G^{\phi}(z_{13}) G^{\lambda}(z_{24}) (G^{\phi}(z_{34}))^{q-1} \tag{C.19}$$

$$K^{\lambda\bar{\phi}\bar{G}\psi}(z_1, z_2, z_3, z_4) = 2J^2 G^{\lambda}(z_{13}) G^{\phi}(z_{24}) (G^{\phi}(z_{34}))^{q-1} \tag{C.20}$$

$$K^{\bar{\psi}G\phi\bar{\lambda}}(z_1, z_2, z_3, z_4) = 2J^2 G^{\psi}(z_{13}) G^{G}(z_{24}) (G^{\phi}(z_{34}))^{q-1} \tag{C.21}$$

$$K^{G\bar{\psi}\bar{\lambda}\phi}(z_1, z_2, z_3, z_4) = 2J^2 G^{G}(z_{13}) G^{\psi}(z_{24}) (G^{\phi}(z_{34}))^{q-1} . \tag{C.22}$$

JHEP12(2018)065

With a similar set of eigenfunctions, the above kernels act as a multiplication of the following

$$k^{\bar{\phi}\lambda\phi\bar{\lambda}}=\frac{(q-1)^2q(\mu q-1)\Gamma\left(-2h_\lambda\right)\Gamma\left(1-2h_\phi\right)\Gamma\left(-h+h_\phi+h_\lambda\right)\Gamma\left(\tilde{h}-\frac{1}{2}+h_\phi+h_\lambda\right)}{\left(\mu q^2-1\right)^2\Gamma\left(2h_\lambda\right)\Gamma\left(2h_\phi\right)\Gamma\left(2-h-h_\phi-h_\lambda\right)\Gamma\left(\tilde{h}+\frac{1}{2}-h_\phi-h_\lambda\right)} \tag{C.23}$$

$$k^{\lambda\bar{\phi}\bar{\lambda}\phi}=\frac{(q-1)^2q(\mu q-1)\Gamma\left(-2h_\lambda\right)\Gamma\left(1-2h_\phi\right)\Gamma\left(-h+h_\phi+h_\lambda\right)\Gamma\left(\tilde{h}-\frac{1}{2}+h_\phi+h_\lambda\right)}{\left(\mu q^2-1\right)^2\Gamma\left(2h_\lambda\right)\Gamma\left(2h_\phi\right)\Gamma\left(2-h-h_\phi-h_\lambda\right)\Gamma\left(\tilde{h}+\frac{1}{2}-h_\phi-h_\lambda\right)} \tag{C.24}$$

$$k^{\bar{\phi}\lambda\psi\bar{G}}=-\frac{(q-1)q\Gamma\left(-2h_\lambda\right)\Gamma\left(1-2h_\phi\right)\Gamma\left(-h+h_\phi+h_\lambda\right)\Gamma\left(\tilde{h}-\frac{1}{2}+h_\phi+h_\lambda\right)}{2\left(\mu q^2-1\right)\Gamma\left(2h_\lambda\right)\Gamma\left(2h_\phi\right)\Gamma\left(2-h-h_\phi-h_\lambda\right)\Gamma\left(\tilde{h}+\frac{1}{2}-h_\phi-h_\lambda\right)} \tag{C.25}$$

$$k^{\lambda\bar{\phi}\bar{G}\psi}=\frac{(q-1)q\Gamma\left(-2h_\lambda\right)\Gamma\left(1-2h_\phi\right)\Gamma\left(-h+h_\phi+h_\lambda\right)\Gamma\left(\tilde{h}-\frac{1}{2}+h_\phi+h_\lambda\right)}{2\left(\mu q^2-1\right)\Gamma\left(2h_\lambda\right)\Gamma\left(2h_\phi\right)\Gamma\left(2-h-h_\phi-h_\lambda\right)\Gamma\left(\tilde{h}+\frac{1}{2}-h_\phi-h_\lambda\right)} \tag{C.26}$$

$$k^{\bar{\psi}G\phi\bar{\lambda}}=\frac{2(q-1)^2q(\mu q-1)\Gamma\left(-2h_\lambda\right)\Gamma\left(1-2h_\phi\right)\Gamma\left(1-h+h_\phi+h_\lambda\right)\Gamma\left(\tilde{h}-\frac{1}{2}+h_\phi+h_\lambda\right)}{\left(\mu q^2-1\right)^3\Gamma\left(1+2h_\lambda\right)\Gamma\left(1+2h_\phi\right)\Gamma\left(2-h-h_\phi-h_\lambda\right)\Gamma\left(\tilde{h}+\frac{1}{2}-h_\phi-h_\lambda\right)} \tag{C.27}$$

$$k^{G\bar{\psi}\bar{\lambda}\phi}=-\frac{2(q-1)^2q(\mu q-1)\Gamma\left(-2h_\lambda\right)\Gamma\left(1-2h_\phi\right)\Gamma\left(1-h+h_\phi+h_\lambda\right)\Gamma\left(\tilde{h}-\frac{1}{2}+h_\phi+h_\lambda\right)}{\left(\mu q^2-1\right)^3\Gamma\left(1+2h_\lambda\right)\Gamma\left(1+2h_\phi\right)\Gamma\left(2-h-h_\phi-h_\lambda\right)\Gamma\left(\tilde{h}-h_\phi-h_\lambda\right)} \tag{C.28}$$

The final eigenvalues are obtained from diagonalizing the following matrix

$$\begin{pmatrix} 0 & 0 & k^{\bar{\phi}\lambda\phi\bar{\lambda}} & k^{\bar{\phi}\lambda\psi\bar{G}} \\ 0 & 0 & k^{\bar{\psi}G\phi\bar{\lambda}} & 0 \\ k^{\lambda\bar{\phi}\bar{\lambda}\phi} & k^{\lambda\bar{\phi}\bar{G}\psi} & 0 & 0 \\ k^{G\bar{\psi}\bar{\lambda}\phi} & 0 & 0 & 0 \end{pmatrix} \tag{C.29}$$

Once more we omit the analytic expression of the eigenvalues but only give the dimensions of the operators that is of most interest to us. This is obtained in a similar manner as above and the result is present in figure 15. From the plot, we indeed observe that there is no half-integer higher-spin operators in the limit (4.1) at any q. These behavior is compatible with the results from the bosonic operator spectrum since we do not expect conserved anti-holomorphic fermionic operators due to the absence of supersymmetry in the left-moving sector. The only conserved operator appears at $\mu = 1$, $s = \frac{3}{2}$, which correspond to the left-moving supercharges emerging as the model develops an enhanced $\mathcal{N} = (2, 2)$ supersymmetry at $\mu = 1$, as we expected.

JHEP12(2018)065

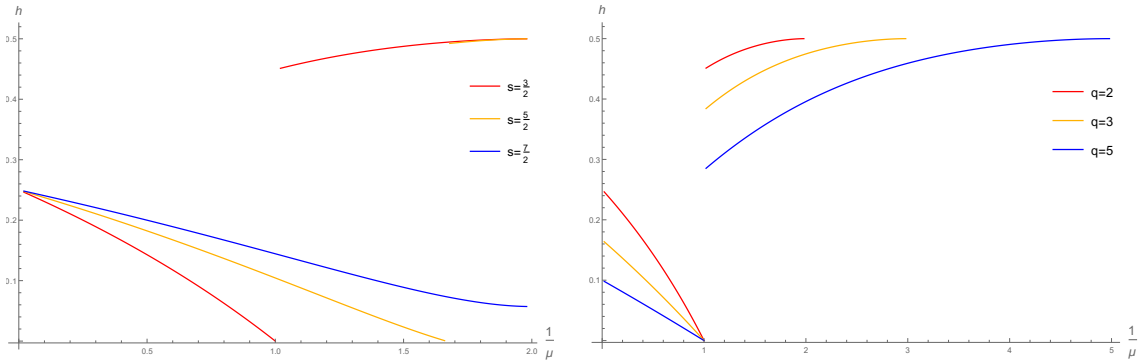

(a) The operators with the lowest dimension in the $\bar{\phi}\lambda$ sector at $q = 2$. There is no higher-spin conserved operators in this sector.

(b) The $\bar{\phi}\lambda$ channel at general q. The curves represent the dimensions of the spin-3 operators in models with different q.

Figure 15. The lowest dimensions of the fermionic operators in the $\langle \phi^i \bar{\lambda}^i \lambda^j \bar{\phi}^j \rangle$ and $\langle \phi^i \bar{\lambda}^i G^j \bar{\psi}^j \rangle$ four point functions. The plots illustrate how does the dimension change as a function of μ. The jumps of the curves are due to the fact that as μ becomes smaller than 1, the branch of operators with the lowest dimension when $\mu \geq 1$ ceases to exist so the operators with the second lowest dimensions become the "lowest" one at $\mu < 1$.

Open Access. This article is distributed under the terms of the Creative Commons Attribution License (CC-BY 4.0), which permits any use, distribution and reproduction in any medium, provided the original author(s) and source are credited.

References

[1] S. Sachdev and J. Ye, *Gapless spin fluid ground state in a random, quantum Heisenberg magnet*, *Phys. Rev. Lett.* **70** (1993) 3339 [cond-mat/9212030] [INSPIRE].

[2] O. Parcollet, A. Georges, G. Kotliar and A. Sengupta, *Overscreened multichannel* SU(N) *Kondo model: Large-N solution and conformal field theory*, *Phys. Rev.* **B 58** (1998) 3794 [cond-mat/9711192] [INSPIRE].

[3] O. Parcollet and A. Georges, *Phys. Rev.* **B 59** (1999) 5341 [cond-mat/9806119].

[4] A. Kitaev, *Hidden correlations in the Hawking radiation and thermal noise*, talk at *KITP Theory Seminar*, 12 February 2015.

[5] A. Kitaev, *A simple model of quantum holography*, talk at *KITP Entangled15*, 7 April 2015.

[6] J. Maldacena and D. Stanford, *Remarks on the Sachdev-Ye-Kitaev model*, *Phys. Rev.* **D 94** (2016) 106002 [arXiv:1604.07818] [INSPIRE].

[7] A. Kitaev and S.J. Suh, *The soft mode in the Sachdev-Ye-Kitaev model and its gravity dual*, *JHEP* **05** (2018) 183 [arXiv:1711.08467] [INSPIRE].

[8] J. Polchinski and V. Rosenhaus, *The Spectrum in the Sachdev-Ye-Kitaev Model*, *JHEP* **04** (2016) 001 [arXiv:1601.06768] [INSPIRE].

[9] A. Jevicki and K. Suzuki, *Bi-Local Holography in the SYK Model: Perturbations*, *JHEP* **11** (2016) 046 [arXiv:1608.07567] [INSPIRE].

JHEP12(2018)065

[10] D.J. Gross and V. Rosenhaus, *The Bulk Dual of SYK: Cubic Couplings*, *JHEP* **05** (2017) 092 [arXiv:1702.08016] [INSPIRE].

[11] D.J. Gross and V. Rosenhaus, *All point correlation functions in SYK*, *JHEP* **12** (2017) 148 [arXiv:1710.08113] [INSPIRE].

[12] D. Bagrets, A. Altland and A. Kamenev, *Sachdev-Ye-Kitaev model as Liouville quantum mechanics*, *Nucl. Phys.* **B 911** (2016) 191 [arXiv:1607.00694] [INSPIRE].

[13] D. Stanford and E. Witten, *Fermionic Localization of the Schwarzian Theory*, *JHEP* **10** (2017) 008 [arXiv:1703.04612] [INSPIRE].

[14] T.G. Mertens, G.J. Turiaci and H.L. Verlinde, *Solving the Schwarzian via the Conformal Bootstrap*, *JHEP* **08** (2017) 136 [arXiv:1705.08408] [INSPIRE].

[15] A. Strominger, *AdS_2 quantum gravity and string theory*, *JHEP* **01** (1999) 007 [hep-th/9809027] [INSPIRE].

[16] J.M. Maldacena, J. Michelson and A. Strominger, *Anti-de Sitter fragmentation*, *JHEP* **02** (1999) 011 [hep-th/9812073] [INSPIRE].

[17] A. Almheiri and J. Polchinski, *Models of AdS_2 backreaction and holography*, *JHEP* **11** (2015) 014 [arXiv:1402.6334] [INSPIRE].

[18] J. Maldacena, D. Stanford and Z. Yang, *Conformal symmetry and its breaking in two dimensional Nearly Anti-de-Sitter space*, *PTEP* **2016** (2016) 12C104 [arXiv:1606.01857] [INSPIRE].

[19] J. Engelsöy, T.G. Mertens and H. Verlinde, *An investigation of AdS_2 backreaction and holography*, *JHEP* **07** (2016) 139 [arXiv:1606.03438] [INSPIRE].

[20] M. Cvetič and I. Papadimitriou, *AdS_2 holographic dictionary*, *JHEP* **12** (2016) 008 [*Erratum ibid.* **01** (2017) 120] [arXiv:1608.07018] [INSPIRE].

[21] D. Grumiller, R. McNees, J. Salzer, C. Valcárcel and D. Vassilevich, *Menagerie of AdS_2 boundary conditions*, *JHEP* **10** (2017) 203 [arXiv:1708.08471] [INSPIRE].

[22] J. Maldacena and X.-L. Qi, *Eternal traversable wormhole*, arXiv:1804.00491 [INSPIRE].

[23] D. Bagrets, A. Altland and A. Kamenev, *Power-law out of time order correlation functions in the SYK model*, *Nucl. Phys.* **B 921** (2017) 727 [arXiv:1702.08902] [INSPIRE].

[24] S.H. Shenker and D. Stanford, *Black holes and the butterfly effect*, *JHEP* **03** (2014) 067 [arXiv:1306.0622] [INSPIRE].

[25] S.H. Shenker and D. Stanford, *Stringy effects in scrambling*, *JHEP* **05** (2015) 132 [arXiv:1412.6087] [INSPIRE].

[26] J. Maldacena, S.H. Shenker and D. Stanford, *A bound on chaos*, *JHEP* **08** (2016) 106 [arXiv:1503.01409] [INSPIRE].

[27] K. Jensen, *Chaos in AdS_2 Holography*, *Phys. Rev. Lett.* **117** (2016) 111601 [arXiv:1605.06098] [INSPIRE].

[28] S. Sachdev, *Holographic metals and the fractionalized Fermi liquid*, *Phys. Rev. Lett.* **105** (2010) 151602 [arXiv:1006.3794] [INSPIRE].

[29] S. Sachdev, *Bekenstein-Hawking Entropy and Strange Metals*, *Phys. Rev.* **X 5** (2015) 041025 [arXiv:1506.05111] [INSPIRE].

[30] W. Fu and S. Sachdev, *Numerical study of fermion and boson models with infinite-range random interactions*, *Phys. Rev.* **B 94** (2016) 035135 [arXiv:1603.05246] [INSPIRE].

JHEP12(2018)065

[31] A. Jevicki, K. Suzuki and J. Yoon, *Bi-Local Holography in the SYK Model*, *JHEP* **07** (2016) 007 [arXiv:1603.06246] [INSPIRE].

[32] L. García-Álvarez, I.L. Egusquiza, L. Lamata, A. del Campo, J. Sonner and E. Solano, *Digital Quantum Simulation of Minimal AdS/CFT*, *Phys. Rev. Lett.* **119** (2017) 040501 [arXiv:1607.08560] [INSPIRE].

[33] A.M. García-García and J.J.M. Verbaarschot, *Spectral and thermodynamic properties of the Sachdev-Ye-Kitaev model*, *Phys. Rev.* **D 94** (2016) 126010 [arXiv:1610.03816] [INSPIRE].

[34] J.S. Cotler et al., *Black Holes and Random Matrices*, *JHEP* **05** (2017) 118 [*Erratum ibid.* **09** (2018) 002] [arXiv:1611.04650] [INSPIRE].

[35] A.M. García-García and J.J.M. Verbaarschot, *Analytical Spectral Density of the Sachdev-Ye-Kitaev Model at finite N*, *Phys. Rev.* **D 96** (2017) 066012 [arXiv:1701.06593] [INSPIRE].

[36] I. Kourkoulou and J. Maldacena, *Pure states in the SYK model and nearly-AdS_2 gravity*, arXiv:1707.02325 [INSPIRE].

[37] J. Sonner and M. Vielma, *Eigenstate thermalization in the Sachdev-Ye-Kitaev model*, *JHEP* **11** (2017) 149 [arXiv:1707.08013] [INSPIRE].

[38] A.M. García-García, Y. Jia and J.J.M. Verbaarschot, *Exact moments of the Sachdev-Ye-Kitaev model up to order $1/N^2$*, *JHEP* **04** (2018) 146 [arXiv:1801.02696] [INSPIRE].

[39] C. Peng, *Vector models and generalized SYK models*, *JHEP* **05** (2017) 129 [arXiv:1704.04223] [INSPIRE].

[40] S. Banerjee and E. Altman, *Solvable model for a dynamical quantum phase transition from fast to slow scrambling*, *Phys. Rev.* **B 95** (2017) 134302 [arXiv:1610.04619] [INSPIRE].

[41] Z. Bi, C.-M. Jian, Y.-Z. You, K.A. Pawlak and C. Xu, *Instability of the non-Fermi liquid state of the Sachdev-Ye-Kitaev Model*, *Phys. Rev.* **B 95** (2017) 205105 [arXiv:1701.07081] [INSPIRE].

[42] C.-M. Jian, Z. Bi and C. Xu, *A model for continuous thermal Metal to Insulator Transition*, *Phys. Rev.* **B 96** (2017) 115122 [arXiv:1703.07793] [INSPIRE].

[43] X.-Y. Song, C.-M. Jian and L. Balents, *A strongly correlated metal built from Sachdev-Ye-Kitaev modelsStrongly Correlated Metal Built from Sachdev-Ye-Kitaev Models*, *Phys. Rev. Lett.* **119** (2017) 216601 [arXiv:1705.00117] [INSPIRE].

[44] Z. Luo et al., *Observing Fermion Pair Instability of the Sachdev-Ye-Kitaev Model on a Quantum Spin Simulator*, arXiv:1712.06458 [INSPIRE].

[45] T. Nosaka, D. Rosa and J. Yoon, *The Thouless time for mass-deformed SYK*, *JHEP* **09** (2018) 041 [arXiv:1804.09934] [INSPIRE].

[46] S. Mondal, *Super-maximal chaos and instability*, arXiv:1801.09669 [INSPIRE].

[47] D.J. Gross and V. Rosenhaus, *A line of CFTs: from generalized free fields to SYK*, *JHEP* **07** (2017) 086 [arXiv:1706.07015] [INSPIRE].

[48] M. Taylor, *Generalized conformal structure, dilaton gravity and SYK*, *JHEP* **01** (2018) 010 [arXiv:1706.07812] [INSPIRE].

[49] S.R. Das, A. Ghosh, A. Jevicki and K. Suzuki, *Three Dimensional View of Arbitrary q SYK models*, *JHEP* **02** (2018) 162 [arXiv:1711.09839] [INSPIRE].

JHEP12(2018)065

[50] S.R. Das, A. Ghosh, A. Jevicki and K. Suzuki, *Space-Time in the SYK Model*, *JHEP* **07** (2018) 184 [arXiv:1712.02725] [INSPIRE].

[51] J. Maldacena, D. Stanford and Z. Yang, *Fortsch. Phys.* **65** (2017) 1700034.

[52] K. Murata, *Fast scrambling in holographic Einstein-Podolsky-Rosen pair*, *JHEP* **11** (2017) 049 [arXiv:1708.09493] [INSPIRE].

[53] J. de Boer, E. Llabrés, J.F. Pedraza and D. Vegh, *Chaotic strings in AdS/CFT*, *Phys. Rev. Lett.* **120** (2018) 201604 [arXiv:1709.01052] [INSPIRE].

[54] R.-G. Cai, S.-M. Ruan, R.-Q. Yang and Y.-L. Zhang, *The String Worldsheet as the Holographic Dual of SYK State*, arXiv:1709.06297 [INSPIRE].

[55] A. Kitaev, *Notes on* $\widetilde{\mathrm{SL}}(2,\mathbb{R})$ *representations*, arXiv:1711.08169 [INSPIRE].

[56] Y.-H. Qi, Y. Seo, S.-J. Sin and G. Song, *Schwarzian correction to quantum correlation in SYK model*, arXiv:1804.06164 [INSPIRE].

[57] H.A. González, D. Grumiller and J. Salzer, *Towards a bulk description of higher spin SYK*, *JHEP* **05** (2018) 083 [arXiv:1802.01562] [INSPIRE].

[58] G. Tarnopolsky, *On large q expansion in the Sachdev-Ye-Kitaev model*, arXiv:1801.06871 [INSPIRE].

[59] E. Witten, *An SYK-Like Model Without Disorder*, arXiv:1610.09758 [INSPIRE].

[60] R. Gurau, *The complete 1/N expansion of colored tensor models in arbitrary dimension*, *Annales Henri Poincaré* **13** (2012) 399 [arXiv:1102.5759] [INSPIRE].

[61] V. Bonzom, R. Gurau and V. Rivasseau, *Random tensor models in the large N limit: Uncoloring the colored tensor models*, *Phys. Rev.* **D 85** (2012) 084037 [arXiv:1202.3637] [INSPIRE].

[62] S. Carrozza and A. Tanasa, $O(N)$ *Random Tensor Models*, *Lett. Math. Phys.* **106** (2016) 1531 [arXiv:1512.06718] [INSPIRE].

[63] R. Gurau, *The complete* $1/N$ *expansion of a SYK-like tensor model*, *Nucl. Phys.* **B 916** (2017) 386 [arXiv:1611.04032] [INSPIRE].

[64] I.R. Klebanov and G. Tarnopolsky, *Uncolored random tensors, melon diagrams and the Sachdev-Ye-Kitaev models*, *Phys. Rev.* **D 95** (2017) 046004 [arXiv:1611.08915] [INSPIRE].

[65] T. Nishinaka and S. Terashima, *A note on Sachdev-Ye-Kitaev like model without random coupling*, *Nucl. Phys.* **B 926** (2018) 321 [arXiv:1611.10290] [INSPIRE].

[66] C. Krishnan, S. Sanyal and P.N. Bala Subramanian, *Quantum Chaos and Holographic Tensor Models*, *JHEP* **03** (2017) 056 [arXiv:1612.06330] [INSPIRE].

[67] F. Ferrari, *The Large D Limit of Planar Diagrams*, arXiv:1701.01171 [INSPIRE].

[68] R. Gurau, *Quenched equals annealed at leading order in the colored SYK model*, *EPL* **119** (2017) 30003 [arXiv:1702.04228] [INSPIRE].

[69] V. Bonzom, L. Lionni and A. Tanasa, *Diagrammatics of a colored SYK model and of an SYK-like tensor model, leading and next-to-leading orders*, *J. Math. Phys.* **58** (2017) 052301 [arXiv:1702.06944] [INSPIRE].

[70] H. Itoyama, A. Mironov and A. Morozov, *Rainbow tensor model with enhanced symmetry and extreme melonic dominance*, *Phys. Lett.* **B 771** (2017) 180 [arXiv:1703.04983] [INSPIRE].

JHEP12(2018)065

[71] C. Krishnan, K.V.P. Kumar and S. Sanyal, *Random Matrices and Holographic Tensor Models*, *JHEP* **06** (2017) 036 [arXiv:1703.08155] [INSPIRE].

[72] H. Itoyama, A. Mironov and A. Morozov, *Ward identities and combinatorics of rainbow tensor models*, *JHEP* **06** (2017) 115 [arXiv:1704.08648] [INSPIRE].

[73] P. Narayan and J. Yoon, *SYK-like Tensor Models on the Lattice*, *JHEP* **08** (2017) 083 [arXiv:1705.01554] [INSPIRE].

[74] S. Chaudhuri, V.I. Giraldo-Rivera, A. Joseph, R. Loganayagam and J. Yoon, *Abelian Tensor Models on the Lattice*, *Phys. Rev.* **D 97** (2018) 086007 [arXiv:1705.01930] [INSPIRE].

[75] R. Gurau, *The $\imath\epsilon$ prescription in the SYK model*, arXiv:1705.08581 [INSPIRE].

[76] S. Dartois, H. Erbin and S. Mondal, *Conformality of $1/N$ corrections in SYK-like models*, arXiv:1706.00412 [INSPIRE].

[77] I.R. Klebanov and G. Tarnopolsky, *On Large N Limit of Symmetric Traceless Tensor Models*, *JHEP* **10** (2017) 037 [arXiv:1706.00839] [INSPIRE].

[78] A. Mironov and A. Morozov, *Correlators in tensor models from character calculus*, *Phys. Lett.* **B 774** (2017) 210 [arXiv:1706.03667] [INSPIRE].

[79] R. Gurau, *The $1/N$ expansion of tensor models with two symmetric tensors*, *Commun. Math. Phys.* **360** (2018) 985 [arXiv:1706.05328] [INSPIRE].

[80] C. Krishnan and K.V.P. Kumar, *Towards a Finite-N Hologram*, *JHEP* **10** (2017) 099 [arXiv:1706.05364] [INSPIRE].

[81] R. de Mello Koch, R. Mello Koch, D. Gossman and L. Tribelhorn, *Gauge Invariants, Correlators and Holography in Bosonic and Fermionic Tensor Models*, *JHEP* **09** (2017) 011 [arXiv:1707.01455] [INSPIRE].

[82] S. Giombi, I.R. Klebanov and G. Tarnopolsky, *Bosonic tensor models at large N and small ϵ*, *Phys. Rev.* **D 96** (2017) 106014 [arXiv:1707.03866] [INSPIRE].

[83] T. Azeyanagi, F. Ferrari and F.I. Schaposnik Massolo, *Phase Diagram of Planar Matrix Quantum Mechanics, Tensor and Sachdev-Ye-Kitaev Models*, *Phys. Rev. Lett.* **120** (2018) 061602 [arXiv:1707.03431] [INSPIRE].

[84] K. Bulycheva, I.R. Klebanov, A. Milekhin and G. Tarnopolsky, *Spectra of Operators in Large N Tensor Models*, *Phys. Rev.* **D 97** (2018) 026016 [arXiv:1707.09347] [INSPIRE].

[85] S. Choudhury, A. Dey, I. Halder, L. Janagal, S. Minwalla and R. Poojary, *Notes on melonic $O(N)^{q-1}$ tensor models*, *JHEP* **06** (2018) 094 [arXiv:1707.09352] [INSPIRE].

[86] C. Krishnan, K.V. Pavan Kumar and D. Rosa, *Contrasting SYK-like Models*, *JHEP* **01** (2018) 064 [arXiv:1709.06498] [INSPIRE].

[87] T. Azeyanagi, F. Ferrari, P. Gregori, L. Leduc and G. Valette, *More on the New Large D Limit of Matrix Models*, *Annals Phys.* **393** (2018) 308 [arXiv:1710.07263] [INSPIRE].

[88] H. Itoyama, A. Mironov and A. Morozov, *Cut and join operator ring in tensor models*, *Nucl. Phys.* **B 932** (2018) 52 [arXiv:1710.10027] [INSPIRE].

[89] D. Benedetti, S. Carrozza, R. Gurau and A. Sfondrini, *Tensorial Gross-Neveu models*, *JHEP* **01** (2018) 003 [arXiv:1710.10253] [INSPIRE].

[90] N. Halmagyi and S. Mondal, *Tensor Models for Black Hole Probes*, arXiv:1711.04385 [INSPIRE].

JHEP12(2018)065

[91] J. Ben Geloun and V. Rivasseau, *A Renormalizable SYK-type Tensor Field Theory*, *Annales Henri Poincaré* **19** (2018) 3357 [arXiv:1711.05967] [INSPIRE].

[92] D. Benedetti, S. Carrozza, R. Gurau and M. Kolanowski, *The $1/N$ expansion of the symmetric traceless and the antisymmetric tensor models in rank three*, arXiv:1712.00249 [INSPIRE].

[93] D. Benedetti and R. Gurau, *2PI effective action for the SYK model and tensor field theories*, *JHEP* **05** (2018) 156 [arXiv:1802.05500] [INSPIRE].

[94] C. Krishnan and K.V. Pavan Kumar, *Complete Solution of a Gauged Tensor Model*, arXiv:1804.10103 [INSPIRE].

[95] N. Delporte and V. Rivasseau, *The Tensor Track V: Holographic Tensors*, 2018, arXiv:1804.11101 [INSPIRE].

[96] J. Maldacena and A. Milekhin, *To gauge or not to gauge?*, *JHEP* **04** (2018) 084 [arXiv:1802.00428] [INSPIRE].

[97] I.R. Klebanov, A. Milekhin, F. Popov and G. Tarnopolsky, *Spectra of eigenstates in fermionic tensor quantum mechanics*, *Phys. Rev.* **D 97** (2018) 106023 [arXiv:1802.10263] [INSPIRE].

[98] D.J. Gross and V. Rosenhaus, *A Generalization of Sachdev-Ye-Kitaev*, *JHEP* **02** (2017) 093 [arXiv:1610.01569] [INSPIRE].

[99] W. Fu, D. Gaiotto, J. Maldacena and S. Sachdev, *Supersymmetric Sachdev-Ye-Kitaev models*, *Phys. Rev.* **D 95** (2017) 026009 [arXiv:1610.08917] [INSPIRE].

[100] C. Peng, M. Spradlin and A. Volovich, *A Supersymmetric SYK-like Tensor Model*, *JHEP* **05** (2017) 062 [arXiv:1612.03851] [INSPIRE].

[101] J. Murugan, D. Stanford and E. Witten, *More on Supersymmetric and 2d Analogs of the SYK Model*, *JHEP* **08** (2017) 146 [arXiv:1706.05362] [INSPIRE].

[102] C. Peng, M. Spradlin and A. Volovich, *Correlators in the $\mathcal{N} = 2$ Supersymmetric SYK Model*, *JHEP* **10** (2017) 202 [arXiv:1706.06078] [INSPIRE].

[103] N. Sannomiya, H. Katsura and Y. Nakayama, *Supersymmetry breaking and Nambu-Goldstone fermions with cubic dispersion*, *Phys. Rev.* **D 95** (2017) 065001 [arXiv:1612.02285] [INSPIRE].

[104] T. Li, J. Liu, Y. Xin and Y. Zhou, *Supersymmetric SYK model and random matrix theory*, *JHEP* **06** (2017) 111 [arXiv:1702.01738] [INSPIRE].

[105] S. Förste and I. Golla, *Nearly AdS_2 SUGRA and the super-Schwarzian*, *Phys. Lett.* **B 771** (2017) 157 [arXiv:1703.10969] [INSPIRE].

[106] T. Kanazawa and T. Wettig, *Complete random matrix classification of SYK models with $\mathcal{N} = 0$, 1 and 2 supersymmetry*, *JHEP* **09** (2017) 050 [arXiv:1706.03044] [INSPIRE].

[107] N. Hunter-Jones, J. Liu and Y. Zhou, *On thermalization in the SYK and supersymmetric SYK models*, *JHEP* **02** (2018) 142 [arXiv:1710.03012] [INSPIRE].

[108] N. Hunter-Jones and J. Liu, *Chaos and random matrices in supersymmetric SYK*, *JHEP* **05** (2018) 202 [arXiv:1710.08184] [INSPIRE].

[109] P. Narayan and J. Yoon, *Supersymmetric SYK Model with Global Symmetry*, *JHEP* **08** (2018) 159 [arXiv:1712.02647] [INSPIRE].

JHEP12(2018)065

[110] S. Förste, J. Kames-King and M. Wiesner, *Towards the Holographic Dual of $N = 2$ SYK*, *JHEP* **03** (2018) 028 [arXiv:1712.07398] [INSPIRE].

[111] A.M. García-García, Y. Jia and J.J.M. Verbaarschot, *Universality and Thouless energy in the supersymmetric Sachdev-Ye-Kitaev Model*, *Phys. Rev.* **D 97** (2018) 106003 [arXiv:1801.01071] [INSPIRE].

[112] K. Bulycheva, *$\mathcal{N} = 2$ SYK model in the superspace formalism*, *JHEP* **04** (2018) 036 [arXiv:1801.09006] [INSPIRE].

[113] Y. Gu, X.-L. Qi and D. Stanford, *Local criticality, diffusion and chaos in generalized Sachdev-Ye-Kitaev models*, *JHEP* **05** (2017) 125 [arXiv:1609.07832] [INSPIRE].

[114] M. Berkooz, P. Narayan, M. Rozali and J. Simón, *Higher Dimensional Generalizations of the SYK Model*, *JHEP* **01** (2017) 138 [arXiv:1610.02422] [INSPIRE].

[115] R.A. Davison, W. Fu, A. Georges, Y. Gu, K. Jensen and S. Sachdev, *Thermoelectric transport in disordered metals without quasiparticles: The Sachdev-Ye-Kitaev models and holography*, *Phys. Rev.* **B 95** (2017) 155131 [arXiv:1612.00849] [INSPIRE].

[116] G. Turiaci and H. Verlinde, *Towards a 2d QFT Analog of the SYK Model*, *JHEP* **10** (2017) 167 [arXiv:1701.00528] [INSPIRE].

[117] M. Berkooz, P. Narayan, M. Rozali and J. Simón, *Comments on the Random Thirring Model*, *JHEP* **09** (2017) 057 [arXiv:1702.05105] [INSPIRE].

[118] Y. Gu, A. Lucas and X.-L. Qi, *Energy diffusion and the butterfly effect in inhomogeneous Sachdev-Ye-Kitaev chains*, *SciPost Phys.* **2** (2017) 018 [arXiv:1702.08462] [INSPIRE].

[119] S.-K. Jian and H. Yao, *Solvable Sachdev-Ye-Kitaev models in higher dimensions: from diffusion to many-body localization*, *Phys. Rev. Lett.* **119** (2017) 206602 [arXiv:1703.02051] [INSPIRE].

[120] X. Chen, R. Fan, Y. Chen, H. Zhai and P. Zhang, *Competition between Chaotic and Nonchaotic Phases in a Quadratically Coupled Sachdev-Ye-Kitaev Model*, *Phys. Rev. Lett.* **119** (2017) 207603 [arXiv:1705.03406] [INSPIRE].

[121] Y. Chen, H. Zhai and P. Zhang, *Tunable Quantum Chaos in the Sachdev-Ye-Kitaev Model Coupled to a Thermal Bath*, *JHEP* **07** (2017) 150 [arXiv:1705.09818] [INSPIRE].

[122] P. Zhang, *Dispersive Sachdev-Ye-Kitaev model: Band structure and quantum chaos*, *Phys. Rev.* **B 96** (2017) 205138 [arXiv:1707.09589] [INSPIRE].

[123] S.-K. Jian, Z.-Y. Xian and H. Yao, *Quantum criticality and duality in the Sachdev-Ye-Kitaev/AdS_2 chain*, *Phys. Rev.* **B 97** (2018) 205141 [arXiv:1709.02810] [INSPIRE].

[124] D. Simmons-Duffin, D. Stanford and E. Witten, *A spacetime derivation of the Lorentzian OPE inversion formula*, *JHEP* **07** (2018) 085 [arXiv:1711.03816] [INSPIRE].

[125] W. Cai, X.-H. Ge and G.-H. Yang, *Diffusion in higher dimensional SYK model with complex fermions*, *JHEP* **01** (2018) 076 [arXiv:1711.07903] [INSPIRE].

[126] X.-H. Ge, S.-J. Sin, Y. Tian, S.-F. Wu and S.-Y. Wu, *Charged BTZ-like black hole solutions and the diffusivity-butterfly velocity relation*, *JHEP* **01** (2018) 068 [arXiv:1712.00705] [INSPIRE].

[127] K. Bulycheva, *A note on the SYK model with complex fermions*, *JHEP* **12** (2017) 069 [arXiv:1706.07411] [INSPIRE].

JHEP12(2018)065

[128] E. Witten, *Phases of $N = 2$ theories in two-dimensions*, *Nucl. Phys.* **B 403** (1993) 159 [hep-th/9301042] [INSPIRE].

[129] M.R. Gaberdiel, W. Li, C. Peng and H. Zhang, *The supersymmetric affine Yangian*, *JHEP* **05** (2018) 200 [arXiv:1711.07449] [INSPIRE].

[130] M.R. Gaberdiel, W. Li and C. Peng, *Twin-plane-partitions and $\mathcal{N} = 2$ affine Yangian*, arXiv:1807.11304 [INSPIRE].

[131] M. Henneaux, G. Lucena Gómez, J. Park and S.-J. Rey, *Super-W_∞ Asymptotic Symmetry of Higher-Spin AdS_3 Supergravity*, *JHEP* **06** (2012) 037 [arXiv:1203.5152] [INSPIRE].

[132] K. Hanaki and C. Peng, *Symmetries of Holographic Super-Minimal Models*, *JHEP* **08** (2013) 030 [arXiv:1203.5768] [INSPIRE].

[133] C. Peng, *Dualities from higher-spin supergravity*, *JHEP* **03** (2013) 054 [arXiv:1211.6748] [INSPIRE].

[134] M.R. Gaberdiel and C. Peng, *The symmetry of large $\mathcal{N} = 4$ holography*, *JHEP* **05** (2014) 152 [arXiv:1403.2396] [INSPIRE].

[135] M.R. Gaberdiel, R. Gopakumar, W. Li and C. Peng, *Higher Spins and Yangian Symmetries*, *JHEP* **04** (2017) 152 [arXiv:1702.05100] [INSPIRE].

[136] M.R. Gaberdiel, C. Peng and I.G. Zadeh, *Higgsing the stringy higher spin symmetry*, *JHEP* **10** (2015) 101 [arXiv:1506.02045] [INSPIRE].

[137] S.S. Gubser, I.R. Klebanov and A.M. Polyakov, *A semiclassical limit of the gauge/string correspondence*, *Nucl. Phys.* **B 636** (2002) 99 [hep-th/0204051] [INSPIRE].

[138] E. Perlmutter, *Bounding the Space of Holographic CFTs with Chaos*, *JHEP* **10** (2016) 069 [arXiv:1602.08272] [INSPIRE].

[139] N. Seiberg and E. Witten, *The $D1/D5$ system and singular CFT*, *JHEP* **04** (1999) 017 [hep-th/9903224] [INSPIRE].

[140] J.M. Maldacena and H. Ooguri, *Strings in AdS_3 and $\mathrm{SL}(2,\mathbb{R})$ WZW model 1.: The spectrum*, *J. Math. Phys.* **42** (2001) 2929 [hep-th/0001053] [INSPIRE].

[141] O. Aharony, Z. Komargodski and S.S. Razamat, *On the worldsheet theories of strings dual to free large N gauge theories*, *JHEP* **05** (2006) 016 [hep-th/0602226] [INSPIRE].

[142] M.R. Gaberdiel, R. Gopakumar and C. Hull, *Stringy AdS_3 from the worldsheet*, *JHEP* **07** (2017) 090 [arXiv:1704.08665] [INSPIRE].

[143] K. Ferreira, M.R. Gaberdiel and J.I. Jottar, *Higher spins on AdS_3 from the worldsheet*, *JHEP* **07** (2017) 131 [arXiv:1704.08667] [INSPIRE].

[144] G. Giribet, C. Hull, M. Kleban, M. Porrati and E. Rabinovici, *Superstrings on AdS_3 at $k = 1$*, *JHEP* **08** (2018) 204 [arXiv:1803.04420] [INSPIRE].

[145] M.R. Gaberdiel and R. Gopakumar, *Tensionless string spectra on AdS_3*, *JHEP* **05** (2018) 085 [arXiv:1803.04423] [INSPIRE].

[146] M.R. Gaberdiel and R. Gopakumar, *Minimal Model Holography*, *J. Phys.* **A 46** (2013) 214002 [arXiv:1207.6697] [INSPIRE].

[147] C.-M. Chang, S. Minwalla, T. Sharma and X. Yin, *ABJ Triality: from Higher Spin Fields to Strings*, *J. Phys.* **A 46** (2013) 214009 [arXiv:1207.4485] [INSPIRE].

JHEP12(2018)065